Biosynthesis of Silver Nanoparticles from *Foeniculum Vulgare* Leaf Extract for Antimicrobial and Antioxidant Activities

Fasika Dereje Ambecha

A Thesis Submitted to the Department of Applied Chemistry

School of Applied Natural Science

Presented in Partial Fulfillment of the Requirements for the Master of Science Degree in Chemistry (Industrial Chemistry)

Office of Graduate Studies

Adama Science and Technology University

November, 2022

Adama, Ethiopia

Biosynthesis of Silver Nanoparticles from *Foeniculum Vulgare* Leaf Extract for Antimicrobial and Antioxidant Activities

Fasika Dereje Ambecha

Advisor: Defaru Negera (Ph.D)

Co-Advisor: Eneyew Tilahun (M.Sc)

A Thesis Submitted to the Department of Applied Chemistry

School of Applied Natural Science

Presented in Partial Fulfillment of the Requirements for the Master of Science Degree in Industrial chemistry

Office of Graduate Studies

Adama Science and Technology University

November, 2022

Adama, Ethiopia

DECLARATION

I hereby declare that this Master Thesis entitled "**Biosynthesis of Silver Nanoparticles from *Foeniculum Vulgare* Leaf Extract for Antimicrobial and Antioxidant Activities**" is my original work. That is, it has not been submitted for the award of any academic degree, diploma, or certificate in any other university. All sources of materials that are used for this thesis have been duly acknowledged through citation.

_____	_____	_____
Name of the Student	Signature	Date

RECOMMENDATION

We, the advisor(s) of this thesis, hereby certify that we have read the revised version of the thesis entitled **"Biosynthesis of Silver Nanoparticles from *Foeniculum Vulgare* Leaf Extract for Antimicrobial and Antioxidant Activities"** prepared under our guidance by **Fasika Dereje Ambecha** submitted in partial fulfillment of the requirements for the degree of Master's of Science in Chemistry (Industrial Chemistry). Therefore, we recommend the submission of a revised version of the thesis to the department following the applicable procedures.

_____	_____	_____
Major Advisor	Signature	Date
_____	_____	_____
Co-advisor	Signature	Date

APPROVAL PAGE

We, the advisors of the thesis entitled **"Biosynthesis of Silver Nanoparticles from *Foeniculum Vulgare* Leaf Extract for Antimicrobial and Antioxidant Activities"** and developed by Fasika Dereje Ambecha, hereby certify that the recommendation and suggestions made by the board of examiners are appropriately incorporated into the final version of the thesis.

Major Advisor	Signature	Date
Co-advisor	Signature	Date

We, the undersigned, members of the Board of Examiners of the thesis by Fasika Dereje Ambecha have read and evaluated the thesis entitled **" Biosynthesis of Silver Nanoparticles from *Foeniculum Vulgare* Leaf Extract for Antimicrobial and Antioxidant Activities"** and examined the candidate during the open defense. This is, therefore, to certify that the thesis is accepted for partial fulfillment of the requirement of the degree of Master of Science in Industrial chemistry.

Chairperson	Signature	Date
Internal Examiner	Signature	Date
External Examiner	Signature	Date

Finally, approval and acceptance of the thesis are contingent upon the submission of its final copy to the Office of Postgraduate Studies (OPGS) through the Department Graduate Council (DGC) and School Graduate Committee (SGC).

Department Head	Signature	Date
School Dean	Signature	Date
Office of Postgraduate Studies, Dean	Signature	Date

ACKNOWLEDGEMENT

I am grateful to the almighty God for the good health and well-being that was necessary to complete this work and for the successful accomplishment of this academic life. To him alone, I give all the glory. Surely goodness and mercy shall follow me all the days of my life.

First and foremost, I would like to begin with a high sense of adoration of my deep thanks go to my advisor, Dr. Defaru Negera (PhD.) for his guidance, encouragement, and support throughout all aspects of this work. Next, I express my gratitude to co-advisor Mr. Eneyew Tilahun for his kindness, unreserved help, encouragement, and valuable time given to me with deep guidance and appreciation. Without their assistance and dedicated involvement in every step throughout the process, this paper would have never been accomplished. I would like to thank you very much for your support and understanding over these past two years. Also, I would like to give my honorable thanks to Adama Science and Technology University, the school of Applied Natural Science, Department of Applied Chemistry as a whole for giving me a scholarship opportunity.

I would also like to acknowledge Kiflom Gebremedhin, Birhanesh Kolcha, Abate Kasaw, Oliqa Mamo, Ilili Dine, Iman Mustefa, and all the academic staff members and laboratory assistants of the Department of Applied Chemistry, at ASTU who gave me valuable comments, materials, and chemicals for my thesis work.

I would also like to thank the Department of Applied Biology for allowing me to use scanning electron microscopy and conduct Antibacterial Activity Applications, the Department of Materials Science Engineering for allowing me to use XRD instruments, Bahir Dar University for running FTIR spectral analysis and Uv-Vis Spectroscopy, and Haramaya University for conducting Antifungal Activity Applications.

Finally, I must express my very profound gratitude and heartfelt special thanks to my family Dereje Ambecha, Tsige Ayano, Daniel Dereje, and Misrak Dereje who help in all directions for my success, for providing me with unfailing support and continuous encouragement throughout my years of study and for their support in everything I need. This accomplishment would not have been possible without them. Thank you.

Table of Contents

LIST OF TABLES

LIST OF FIGURES

LIST OF ABBREVIATIONS

Ag NPs	Silver Nanoparticles
ATP	Adenosine triphosphate
DLS	Dynamic light scattering
DMSO	Dimethyl Sulphoxide
DNA	Deoxyribonucleic Acid
DPPH	2,2-Diphenyl-1-picrylhydrazyl
FCC	Face-Centered Cubic
FTIR	Fourier Transform Infrared Spectroscopy
FWHM	Full Width at Half Maximum
JCPDS	Joint Committee on Powder Diffraction Standards
MFC	Minimum Fungicidal Concentration
MHA	Muller Hinton Agar
MIC	Minimum Inhibitory Concentration
NADPH	Nicotinamide Adenine Dinucleotide Phosphate
Nm	Nanometer
NMs	Nanomaterials
NPs	Nanoparticles
NSMs	Nanostructured materials
PDA	Potato Dextrose Agar
ROS	Reactive Oxygen Species
RPM	Revolution per Minute

RSA	Radical-Scavenging Assay
SDA	Sabouraud Dextrose Agar
SEM	Scanning Electron Microscopy
SPR	Surface Plasm Resonance
TEM	Transmission Electron Microscopy
USA	United State of America
UV-vis	Ultraviolet-visible spectroscopy
XRD	X-ray Diffraction
ZOI	Zone of Inhibition

ABSTRACT

Ethiopian medicinal plant, Foeniculum vulgare leaf mediated green silver nanoparticles were successfully synthesized for the first time. In this study, silver nanoparticles were biosynthesized by using the leaf extracts of Foeniculum vulgare and 0.1 M of silver nitrate in three different volume ratios of 100 mL:100 mL (1:1), 50 mL:150 mL (1:3), and 150 mL:50 mL (3:1). The biosynthesized silver nanoparticles were characterized by XRD, UV-vis, FTIR, and SEM. The XRD results confirmed that silver nanoparticles were found to exhibit a face-centered cubic phase structure and the sharp and intense peaks at 2θ values of 38.21°, 44.38°, 64.77°, and 77.58° have confirmed the formation of crystalline silver nanoparticles. The band gap energy of biosynthesized silver nanoparticles was found to be 3.23 eV, 3.35 eV, and 3.51 eV for 1:1, 1:3, and 3:1 ratios respectively. FT-IR spectra were recorded for the Foeniculum vulgare leaf extract and for the silver nanoparticles to identify the biomolecules involved in the synthesis process. The SEM images showed a spherical shape for silver nanoparticles. The antimicrobial activity of the biosynthesized silver nanoparticles was screened against two Gram-positive bacteria (Streptococcus pyogenes and Staphylococcus aureus) and two Gram-negative bacteria (Escherichia coli and Pseudomonas aeruginosa) and fungal strains (Aspergillus niger and Candida albicans) using the using Agar disc diffusion method. Results showed that all the studied silver nanoparticles ratios displayed good antibacterial activity compared to amoxicillin which was used as a positive control. Among the three different volume ratios, silver nanoparticles 3:1 ratios shows better performance towards Gram-positive bacteria, due to its smaller average crystalline size and uniform morphology observed in the SEM image relative to the other two ratios of silver nanoparticles. The best antifungal activity was displayed by Aspergillus niger at a 3:1 ratio with a maximum zone of inhibition of 13, 14.8, and 16.8 mm at the concentrations of 15, 20, and 25 mg/mL, respectively. The antioxidant capacity of silver nanoparticles was investigated in vitro by 2, 2-diphenyl-1-picrylhydrazyl (DPPH) assays. DPPH radical scavenging activity displayed 42.4%, 27.3%, and 28.9% inhibition for 1:1, 1:3 and 3:1 silver nanoparticles volume ratios respectively, at 800 μg/mL.

Keywords: Antimicrobial activity, Antioxidant, *Foeniculum vulgare*, and Silver nanoparticles

1. INTRODUCTION

1.1. Background of the Study

Silver nanoparticles are useful nanomaterials that have many applications in different fields. Among various metal nanoparticles, silver has attracted particular attention (Ghotekar et al., 2019). Because of its potential applications in commercial, and its biological area with up-to-date technologies viz. biocidal activity, sensors, catalysis, superconductivity, medicine, environmental remediation, chemical industry, agriculture, and water purification. Hence the applications of Ag NPs include; antibacterial, antioxidant, anti-fungal agent, anti-fouling, anti-biotic, and so on (Abdulsahib, 2021).

Different chemical and physical methods have been utilized in the synthesis of Ag NPs. However, these methods are not safe for the preparation of Ag NPs, due to the presence of hazardous chemicals and these methodologies remain high-cost, where flammable or corrosive reducing agents used. This may pose potential environmental and biological risks (Yaqoob et al., 2020). Because noble metal NPs are widely applied to areas of human contact, and due to the high surface charge and high surface area of NPs, harsh chemicals may remain adsorbed onto NPs. Releasing these chemicals into the environment may cause adverse effects on organisms including microorganisms, plants as well as humans at various trophic levels. Thus, developing environment-friendly protocols is the need of the hour in nanomaterial synthesis. Thus, development of Ag NPs synthesis by the biological method instead of using toxic chemicals is preferable (Irshad et al., 2020). The interest in this field has then shifted toward "green" chemistry and the bio-process approach. The "green" methods for the synthesis and production of nanomaterials used in both industrial applications and scientific research have achieved a massive amount of interest (Huston et al., 2021).

In general, some specific plant parts or whole plants, favorably angiosperm plants (flowering plants, approximately 80 percent of all the known green plants now living), are used for the green synthesis of nanoparticles (Pal et al., 2019). Numerous plant extracts are used for the green synthesis of Ag NPs and *Foeniculum vulgare* is one of the indigenous plants used to synthesize Ag NPs. *Foeniculum vulgare* is derived from the leaves of a small ever-green

perennial found in tropical Africa, Asia, and the southern Mediterranean region (Batsatsashvili et al., 2020). In Ethiopia, the plant is called *Ensilal*. This plant leaf has great nutritional, herbal, and medicinal value. Such bioactivities help to synthesize NPs having lower-dimensional structures less than 100 nm (Badgujar et al., 2014). The presence of active biomolecules in the leaf helps for capping and stabilizing agents in green methodology for efficient metal-based NPs preparation. But none of the previous studies have used the *Foeniculum vulgare* leaf for the biosynthesis of Ag NPs. This thesis is to report such work in Ethiopia. This research aims to present the biosynthesis of Ag NPs using medicinal plant *Foeniculum vulgare* leaf extract to explore the beneficial influence of phytochemicals present around the Ag NPs on bacterial strains and fungal strains to evaluate its antioxidant activity. The biosynthesized Ag NPs were characterized by different techniques and evaluated for antimicrobial and antioxidant properties. Hence, this thesis is believed to have contributed to increasing reports of biosynthesis of Ag NPs as well as in making nanoparticles easily prepared and cheaply available.

1.2. Statement of the Problem

Some rational problems initiate to conduct biosynthesis of Ag NPs using *Foeniculum vulgare* leaf extract and its application for antimicrobial and antioxidant activity. Silver has obtained antimicrobial and antioxidant effects with particular properties of conductivity, stability, effectiveness, and activity. Microbial infectious diseases become a serious health problem that has drawn public attention worldwide as a human health threat that extends to economic and social complications. Bacterial and fungal infectious diseases are major problems in developing countries. They develop microbial resistance methods that traditionally used antimicrobials, which is more difficult for communities to select an appropriate antimicrobial agent. The most problems with microbial infectious diseases are bacterial and fungi infection not only its mortality and morbidity but also in terms of treatment costs, low efficiency of treatment, and insufficient distribution to society. However, controlling these microbial infectious diseases is more difficult today because of the emergence of drug-resistant bacteria, fungi, viruses, *etc*. At the same time, the burden of microbial infectious diseases is high and patients with a resistant infection may be unable to obtain or afford any of the available drugs. For this reason, in underdeveloped and developing countries like Ethiopia, those microbial

infection diseases were serious health hazards, especially for children and old aged people due to the lack of suitable vaccines. Therefore, the synthesis of Ag NPs for potential antioxidant and antimicrobial agents is being considered to fill some of this gap. Different research has been done on the biosynthesis of Ag NPs for antioxidant and antimicrobial applications however, there is a limit on the synthesis of NPs by green methods using medicinal plant extracts. Besides *Foeniculum vulgare* leaf is harmless, cheap, and easily available around the local area. This study carried out to synthesize Ag NPs by biological method from silver nitrate salt using extracts of *Foeniculum vulgare* leaf as reducing and stabilizing agents and its antimicrobial activity on some bacteria and fungi including its antioxidant activity. The aims of this research were the synthesis of Ag NPs using the biological method in the presence of the extract of *Foeniculum vulgare* leaf and the evaluation of its application for antimicrobial and antioxidant activity.

1.3. Objectives

1.3.1. General objective

The general objective of this research is the biosynthesis and characterization of silver nanoparticles from *Foeniculum vulgare* leaf extract for antimicrobial and antioxidant activities.

1.3.2. Specific objectives

The specific objectives of this research work were;

- To carry out a phytochemical test of the leaf of *Foeniculum vulgare*.
- To biosynthesize Ag NPs silver nanoparticles 1:1, 1:3, and 3:1 volume ratios of *Foeniculum vulgare* leaf extract vs from its silver nitrate precursor.
- To characterize the biosynthesized silver nanoparticles using XRD, UV-Vis, FTIR, and SEM.
- To consider the antibacterial activities of silver nanoparticles against *Staphylococcus aureus, Streptococcus pyogenes*, *Pseudomonas aeuruginosa,* and *Escherichia coli.*
- To consider the antifungal activities of silver nanoparticles against *Aspergillus niger* and *Candida Albicans*.

- To consider the radical scavenging activities of silver nanoparticles using DPPH assay.

1.4. Significance of the Study

This work is expected to have its own contribution to the biosynthesis and application of Ag NPs. It gives information to the community about the biosynthesis of the Ag NPs using locally available plant *Foeniculum vulgare* leaf. It also gives information on how to produce nanoparticles that have enhanced performance quality at low cost, harmless, and give basic knowledge about Ag NPs. The outcome of this research can have a considerable effect on research and even on industrial activities as it serves as a basis for any scientific investigations of Ag NPs. It can also serve as background information for a researcher who wants to conduct further study on the topic under study and it provides information to prospects about various potential applications of the *Foeniculum vulgare* plant for synthesizing Ag NPs using the conventional synthesizing process. Anticipated as one possible means of biological synthesis of Ag NPs of desired quality with low cost, environmental eco-friendly, and convenient methods of preparation so that the harmful or risky nature of the chemical methods of synthesizing Ag NPs can be avoided. Using easily available Ag NPs is also expected to make the protection and removal of bacterial microbes easy and effective. Its applications are a very promising, efficient, and cost-effective method for remediating this environmental health concern. It is believed that this work has a positive impact on increasing the number of available research works dealing with silver nanoparticles biosynthesis and its antimicrobial and antioxidant activity.

1.5. Scope of the Study

The scope of this research work involved the biosynthesis of Ag NPs by using *Foeniculum vulgare* leaf extract. Accordingly, it proved some of the bioactive substances that can be derived from leaf extracts. Besides, followed by characterizing the biosynthesized Ag NPs using XRD, UV-vis, FT-IR, and SEM. Finally, it evaluated the efficiency of antioxidant and antimicrobial properties of Ag NPs biosynthesized against selected bacterial strains: Gram-negative bacteria *E. coli, P. aeuruginosa,* and Gram-positive bacteria *S. aureus, S. pyogenes,* and fungal strain *Aspergillus niger* and *Candida Albicans.*

2. LITERATURE REVIEW

2.1. Nanoparticles

Nowadays, nanotechnology has been expanding rapidly in recent years, impacting diverse areas such as the economy and the environment. The development of nanotechnology has resulted in a growing public debate on the toxicity and environmental impact of direct and indirect exposures to NPs (Babatunde et al., 2019). NPs are the fundamental building blocks of nanoscience and nanotechnology. NPs are particles with an interfacial layer and a maximum size range of 100 nm. NPs, which are defined as a collection of atoms bonded together with a structural radius of less than 100 nm, are a link between bulk materials and atomic or molecular structures (Barhoum et al., 2019). They have completely new or improved properties that differ significantly from those of larger particles. When compared to larger bulk materials, NPs have distinct properties such as size, shape, dispersion, and surface morphology. NPs are available in a variety of shapes and sizes, such as spheres, cylinders, platelets, tubes, and others (Paper & Haider, 2018).

2.2. Silver Nanoparticles and its Properties

2.2.1. Electrical properties

Silver, due to its unique electrical properties can be used in electronic devices. Ag NPs can be used to make electronic devices. The electrical conductivity of Ag NPs ranging in size from 4 to 12 nm and grown in glass-ceramic was investigated (Mohd Radzuan et al., 2017). Silver has the highest electrical conductivity, thermal conductivity, ductility, and contact resistance of any metal. As for metallic silver form, it is insoluble in water, but its metallic salts such as $AgNO_3$, and AgCl, are water-soluble the electrons that cannot move freely at nanolevel and their motion became restricted, this confinement at the nanoscale resulted in the changes in electrical properties, such as the bulk conductor/semiconductor materials behaving as superconductors or conductors at the nanoscale. Similarly, nanosilver (of size less than 10 nm) cannot conduct electricity. Other applications include data storage, devices, optoelectronics, nanoelectronics, and soon (Consumption et al., 2017).

2.2.2. Morphologies and sizes

The morphological change is the result of a complex interaction of molecular surface and crystalline properties. The antibacterial activity is enhanced by the large surface-to-volume ratio of that of a spherical shape. For example, when Ag NPs can interact with bacterial cells, smaller particles that have a large surface area are the most effective as antibacterial than larger particles (Pandey et al., 2012). Using various reducing and capping agents, silver nanoparticles of different sizes and morphologies were obtained by Shervani *et al.* analyzed the effects of the reducing agent on Ag NPs sizes at ambient temperature. It was found that spherical silver particles of 8 and 24 nm diameter were obtained when applying the reducing agent to the silver salt in liquid crystalline pluronic (Consumption et al., 2017).

2.2.3. Crystalline structures

According to *Khan et al*. study the XRD was done to determine the crystalline nature of Ag NPs and the resulting peaks were found at 37.90°, 44.05°, 64.25°, and 77.20° representing (111), (200), (220) and (311) face-centered cubic structure of silver which were compared with the standard powder diffraction card of Joint Committee on Powder Diffraction Standards (JCPDS), silver file No. 04–0783. The average particle size was calculated by the Debye-Scherer equation where full width at half maximum (FWHM) data was used. The average particle size estimated was approximately 6.43 nm (Khan et al., 2018). *Esmaile et al.* reported the crystalline structure of the Ag NPs was examined by XRD and the XRD patterns of the nanoparticles were obtained at optimum conditions. It is evident that the peaks of (111), (200), (220), and (311) at 2θ = 38.06, 44.30, 64.40, and 77.36 respectively, are related to the FCC structure of the Ag NPs (ICCD No. 01-071-4613), and proves the successful synthesis of the nanoparticles (Esmaile et al., 2020).

2.2.4. Chemical properties

Silver has the chemical symbol Ag and the atomic number 47. It has a melting temperature of approximately 961.78°C and a boiling temperature of approximately 216.2°C. Silver can occur naturally in the Ag^0, Ag^+, Ag^{2+}, and Ag^{3+} oxidation states. Ag^0 and Ag^{2+} are the most abundant, while Ag^{3+} is unstable in the aquatic environment. Silver has two stable isotopes, ^{107}Ag and

^{109}Ag, which exist in equal proportions (Rawat, 2016). Metallic silver is insoluble in water, but metallic salts such as silver nitrate and silver chloride are soluble in water (Khodadadi et al., 2021).

2.2.5. Optical properties

When Ag NPs are exposed to a specific wavelength of light, the light's oscillating electromagnetic field induces a collective coherent oscillation of the free electrons, resulting in charge separation concerning the ionic lattice and the formation of a dipole oscillation along the direction of the light's electric field. The amplitude of the oscillation reaches its peak at a specific frequency, which is known as surface plasmon resonance (SPR) (Shrivas et al., 2016). Controlling the particle size, shape, and refractive index near the particle surface can alter the absorption and scattering properties of Ag NPs. For example, smaller nanoparticles mostly absorb light and have peaks near 400 nm, while larger nanoparticles exhibit increased scattering and have peaks that broaden and shift towards longer wavelengths. Furthermore, when particles aggregate and the conduction electrons near each particle's surface become delocalized, the optical properties of Ag NPs can change (Salem et al., 2016). Alternatively, Martínez-Castañón reported that the synthesized Ag NPs were characterized in various sizes using gallic acid via an aqueous chemical reduction method. Their research found that spherical Ag NPs with a size of 7 nm have a surface plasmon resonance at 410 nm, while those with a size of 29 nm have a resonance at 425 nm. Furthermore, Ag NPs with a size of 89 nm exhibited a wider band with a maximum of 490 nm. It was noticed that the width of surface plasmon resonance was related to the size distributions of nanoparticles (Mlalila et al., 2017).

2.3. Approaches for the Synthesis of Silver Nanoparticles

In general, Ag NPs can be produced using one of two methods: the bottom-up approach or the top-down approach (Paula et al., 2020). The size of silver metal in its bulk form is mechanically reduced to the nano-scale in the top-down (physical) approach (Reverberi et al., 2019). The bottom-up (chemical and biological) approach is also known as the self-assembly technique, Ag NPs are obtained from their basic building blocks, which react to produce Ag NPs of the desired shape and size and include dissolution of silver salt into a solvent, reduction of silver ions to their element using the addition of a reducing agent, and then stabilization of the

forming Ag NPs using a stabilizing agent to prevent non - specific binding (Siddiqi et al., 2018). The Figure 1 shows the summary of synthesis methods of nanoparticles including silver nanoparticles.

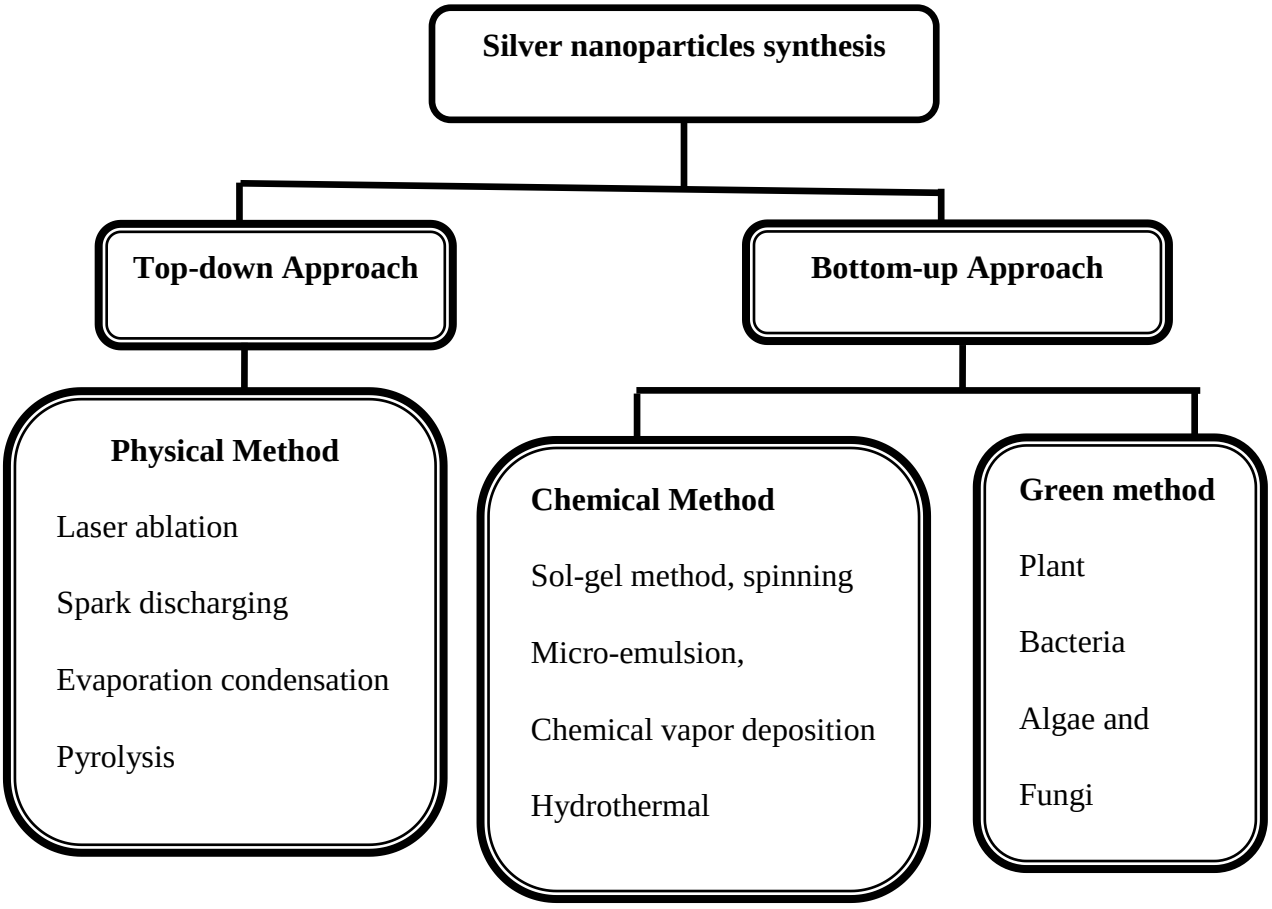

Figure 1. General synthesis methods of silver nanoparticles (Patra & Baek, 2014).

2.3.1. Physical method

For the synthesis of Ag NPs, conventional physical methods such as spark discharging and pyrolysis were used. The most important physical approaches are evaporation-condensation and laser ablation. In comparison to chemical processes, the absence of solvent contamination in the prepared thin films and the uniformity of nanoparticles distribution are advantages of physical synthesis methods. Furthermore, physical methods are faster; radiation is used as a reducing agent; and there is no involvement of toxic chemicals (Yusuf, 2019). The physical methods use high thermal energy and high pressure for the synthesis (Thiagarajan et al., 2017).

The other physical synthesis methods of Ag NPs are achieved by evaporation condensation using in a tube furnace at atmospheric pressure. The source of material in a boat is a spot centered in the furnace and vaporized against a carrier gas. The physical synthesis of Ag NPs at atmospheric pressure has some drawbacks. For example, the tube furnace takes up a lot of space, consumes a lot of energy while raising the temperature around the source material, and takes a long time to achieve thermal stability (Kim et al., 2017). The use of a typical tube furnace in this method has involved power consumption and chumble a lot of energy trouble in raising the temperature around the source material to attain a stable operating temperature (Rafique et al., 2017).

2.3.2. Chemical method

Some of the commonly used chemical methods are solvothermal synthesis, chemical reduction, Co-Precipitation, sol-gel technique, microemulsion, Pyrolysis, chemical vapor synthesis and hydrothermal methods that are used to synthesize Ag NPs in different sizes, shapes, and morphological structures (Vega-Baudrit et al., 2019). The most common method for the synthesis of Ag NPs is chemical reduction, which is based on the reduction of aqueous silver nitrate in an appropriate operating medium with chemical reductants such as sodium citrate or branched polyethyleneimine. Sodium citrate, ascorbate, sodium borohydride ($NaBH_4$), elemental hydrogen, polyol process, Tollens reagent, N, N-dimethyl formamide (DMF), and polyethylene glycol-block copolymers are some of the commonly used reducing agents in this method for the reduction of silver ions (Ag^+) in aqueous or non-aqueous solutions (Quintero-quiroz et al., 2019). Chemical reduction is the most commonly used method for producing stable colloidal dispersions of Ag NPs in water or organic solvents. Silver ions (Ag^+) are reduced in an aqueous solution to produce colloidal silver with particle diameters of several nanometers. Capping agents are additionally used for size stabilization of the nanoparticle. The reducing agents reduce Ag^+ and conduct the formation of metallic Silver Ag^0. Following this, agglomeration changes into oligomeric clusters, resulting in the formation of metallic colloidal Ag NPs (Núñez et al., 2018).

When silver nitrate dissolves, it produces a positive silver ion (Ag^+) and a negative nitrate ion (NO_3^-). To convert silver ions into solid silver, they must be reduced by absorbing an electron

from a donor. Equation 1 shows an illustration of the reduction of silver ions by the addition of an electron. Equation 2 depicts the reduction of (Ag^+) in an ethanol solution. After the silver germ is formed, it begins to grow and continues to grow until the equilibrium between the final nanoparticles and the solution (Ag^+) is reached (Chou et al., 2005).

$$Ag^+ (aq) + e^- \rightarrow Ag(s) \quad (1)$$

$$2Ag^+ (aq) + C_2H_5OH + H_2O \rightarrow 2Ag(s) + C_2H_5O_2^- + 3H^+ \quad (2)$$

The chemical reduction method of Ag NPs synthesis using sodium borohydride as a reducing agent is given below.

$$AgNO_3 + NaBH_4 \rightarrow Ag + \frac{1}{2}H_2 + \frac{1}{2}B_2H_6 + NaNO_3 \quad (3)$$

Also, Ag NPs can be prepared inside microemulsion. The initial spatial separation of reactants (metal precursor and reducing agent) in two immiscible phases is the basis for the synthesis of Ag NPs in two-phase aqueous organic systems. The interface between the two liquids and the intensity of interphase transport between the aqueous and organic phases, which is mediated by a quaternary alkylammonium salt, control the rate of subsequent interaction between the metal precursor and the reducing agent. Gao *et al* reported the development of the Ag NPs through two steps: first, the Ag^+ ions were reduced by $NaBH_4$ to give Ag NPs Ag^+, and then ascorbic acid was added to reduce the remaining Ag^+ ions. The growth of Ag NPs can be enhanced by increasing the concentration of ascorbic acid. However, the use of sodium citrate, a weaker reducing agent compared to ascorbic acid, generates Ag NPs of a slightly larger average diameter of 30 nm, in the presence of glycerin at a temperature of 100^0C (Hasnain et al., 2019).

In addition to chemical methods, electrochemical and sonochemical methods for synthesizing silver nanoparticles are rapidly growing. Sanchez et al. employed an electrochemical method that involved dissolving a silver anode in an acetonitrile solution containing tetrabutylammonium salt to obtain Ag NPs with sizes ranging from 2 to 7 nm, as confirmed by TEM (Rodrı, 2000). As the current density increases, the overpotential increases, and the size of the silver decreases. Similarly, Wadkar et al. synthesized Ag NPs ranging in size from 2 to

10 nm by electrochemical dissolution of the silver anode in dimethyl sulfoxide (DMSO) without the use of any stabilizing agent. The exceptional stability of Ag NPs, even in the absence of stabilizing agents, was due to the formation of the Ag(I) DMSO complex on particle surfaces as confirmed by FTIR, thermal analysis, and fluorescence spectroscopy (Li et al., 2016)**.** Moreover, Kumar *et al*. reported a novel method for synthesizing colloidal Ag NPs under ultrasound irradiation (sonication) by using a polysaccharide, starch, as both a reducing and a stabilizing agent (B. Kumar et al., 2014)**.** The formation of spherical, polydisperse, and partially crystalline Ag NPs was revealed by spectroscopic analyses (23-97 nm). Thus, sonochemical methods provide a nontoxic, environmentally friendly, and cost-effective method for synthesizing Ag NPs at room temperature, but their size-control ability is typically less than that of electrochemical methods (Jiang et al., 2020).

2.3.3. Green/biological method

Biological methods can be used to synthesize Ag NPs without the use of any harsh, toxic, and expensive chemical substances (Nzekekwu & Abosede, 2019).As well as, this method does not need high pressure, temperature, energy, and toxic chemicals. Green synthesis can be classified as (a) utilization of microorganisms like fungi, yeasts (eukaryotes), and bacteria, (b) use of plants tissues (leaves, fruit, latex, peel, flower, root, stem, etc.), and plant extracts (c) use of templates like membranes, viruses DNA, and diatoms. Several plants are being currently investigated for their role in the synthesis of Ag NPs (Thangavelu et al., 2018). Therefore there is more focus on Ag NPs synthesis using natural resources such as plants and microbes which is termed “green synthesis” (J. Singh et al., 2018).

2.3.3.1. Synthesis of Silver Nanoparticles by Using Bacteria

The *Pseudomonas stutzeri* strain was cultured in high concentrations of silver nitrates/minerals and provided the first evidence of bacteria synthesizing Ag NPs (Vanlalveni et al., 2018). The use of bacteria selected through green synthesis makes it flexible, inexpensive, and suitable for large-scale production (Roy et al., 2019). There is also another aspect that though these organisms can grow at lower concentrations, their exposure to higher concentrations of metal ions can induce toxicity. The most widely accepted mechanism of silver biosynthesis is the

presence of the nitrate reductase enzyme. The enzyme converts nitrate into nitrite. The presence of alpha-nicotinamide adenine dinucleotide phosphate reduced form (NADPH) - dependent nitrate reductase in vitro silver production utilizing bacteria would remove the downstream processing step that is required in other circumstances. Biosorption of metals by Gram-negative and Gram-positive bacteria revealed the manufacture of nanoparticles before the widespread use of this biological technique; however, the nanomaterials generated were aggregates, not nanoparticles (Ibrahim et al., 2019)**.** Similarly, the core idea behind synthesizing Ag NPs in *Bacillus licheniformis* was to use a cell-free supernatant generated after separating *Bacillus licheniformis* cells in the form of a metabolite (arginase) produced by the fermentation process (Momin et al., 2019)**.** As a stabilizing agent for the biosynthesis of Ag NPs, cell-free supernatants of *Bacillus amyloliquefaciens* can be used (Samuel et al., 2019).

2.3.3.2. Synthesis of Silver Nanoparticles by using Fungi

Fungi can produce more Ag NPs than bacteria because they can release more proteins, which immediately translates to increased nanoparticles productivity. The fungal-mediated mechanism of Ag NPs synthesis where cell wall, cell membrane, and other biomolecules such as proteins and enzymes play important roles in nanoparticles formation is linked to the cell wall (electron shuttle quinones) (Salunke et al., 2016). Both intra- and extracellular synthesis can be seen in *Fusarium spp*., where the electrostatic interaction in the cell surface traps the silver ion, and the silver ions are reduced by the catalytic activity of the enzymes present in the cell wall. Due to the electrostatic interaction between the free cysteine residues or amino groups, the fungal proteins and peptides stabilized the formed Ag NPs (Guilger-casagrande & Lima, 2019).

The following steps are reported to be involved in the production of Ag NPs by fungi: trapping of Ag+ ions on the surface of fungal cells and subsequent silver ion reduction by enzymes present in the fungal system (Basavaraja et al., 2008). The stabilization of Ag NPs by proteins improves the stability of the nanoparticle solution. Extracellular enzymes such as naphthoquinones and anthraquinones are thought to contribute to the reduction process. Ag NPs (5-50 nm) could, for example, be generated extracellularly using *Fusarium oxysporum*, with no signs of flocculation even a month after the reaction. Using *Aspergillus flavus*, stable

Ag NPs can be made (Prabhu & Poulose, 2012). Supernatants of *Candida albicans* and *Saccharomyces sp.* are also efficient for Ag NPs synthesis with sizes ranging from 2 to 7.3 nm (Boobalan et al., 2018)**.** Ag NPs of different sizes have been obtained from extracellular synthesis using different fungi: *Aspergillus niger*, Ag NPs -Asp (40 ± 5) (Felici & Raba, 2015)**.**

2.3.3.4. Synthesis of Silver Nanoparticles by using Plant Extracts

Extracts from various plant sources resulted in Ag NPs of different sizes; these plant sources included the bark of *Salacia chinensis* (40- 80 nm), the leaf extract of *Brassica rapa L*. (5.7–24.4 nm), the leaf extracts of the medicinal plants *Semecarpus anacardium, Glochidion lanceolarium, Bridelia retusa*, and *Enicostemma axillare (Lam.)* (15-20 nm), and the extract of *Cannabis sativa* (20–40 nm), which were used as reducing, stabilizing, and capping agents. Plant-assisted reduction and stability due to phytochemicals is the key mechanism suggested for the procedure (Jadhav et al., 2018)**.** The major advantage of using plant extracts for Ag NPs synthesis is that they are easily available, simple, efficient, safe, and nontoxic in most cases, have a broad variety of metabolites that can aid in the reduction of silver ions, and are quicker than microbes in the synthesis (Meena et al., 2020). The synthesis process is prepared by the addition of extract obtained from various plant parts such as flowers, stems, leaves, roots, and fruits into the aqueous solution of metal ions. The main mechanism considered for the process is the plant-assisted reduction and stabilization due to phytochemicals. Proteins, terpenoids, enzymes, flavones, polysaccharides, amides, sugars, ketones, aldehydes, and carboxylic acids are the main phytochemicals present in plants and these are responsible for the bioreduction of nanoparticles. It has been speculated that polyphenols such as alkaloids and polysaccharides in plant extracts might be responsible for reducing $AgNO_3$ to Ag NPs (Meena et al., 2020). The phytochemicals found in plant leaf extracts can reduce metal ions in a short period as compared to microbes such as fungi and bacteria, which demands a longer incubation time (Din et al., 2017). Ahmed et al. suggested that the phytochemicals are involved directly in the reduction of the ions and formation of silver nanoparticles (Aisida et al., 2019).

Similarly, by changing the plant extract concentration (extract: salt solution ratio), temperature, and pH of the reaction mixture, the average size of Ag NPs can be controlled. Tea leaf extract can be used to synthesize Ag NPs, and the size could be controlled by variation of the

concentration of both extract solution and the salt solution; thus, resulting in the Ag NPs formed being safe for human beings (Allah & Mohanta, 2020). A low concentration of extract can reduce silver ions but cannot prevent agglomeration of nanoparticles due to a lack of biomolecules that act as capping agents. In the case of a higher concentration, the biomolecules act as both reducing and capping agents, and a higher concentration of extract is also responsible for the formation of symmetrical silver nanoparticles. Figure 2 shows the chemical structure of silver nitrate which can be used to synthesize Ag NPs.

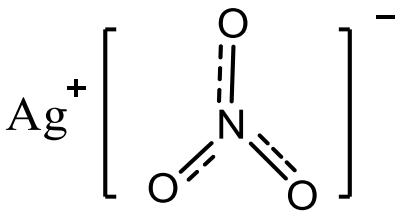

Figure 2.Chemical structure of silver nitrate.

The silver ion in silver nitrate undergoes reduction to become a silver molecule. The formula is shown in the Equation below.

$$Ag^{+} \longrightarrow Ag^{0}$$

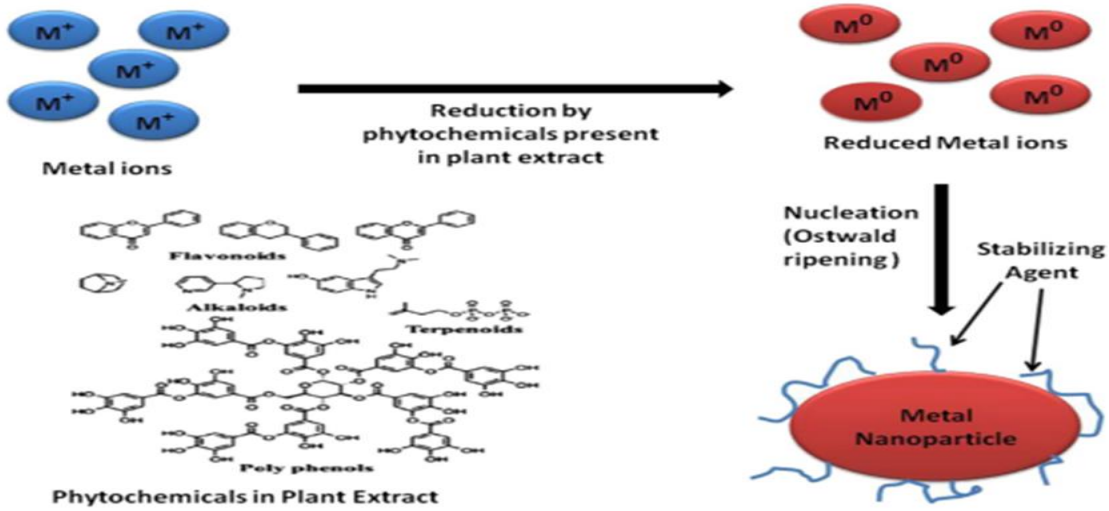

Figure 3. Mechanism of nanoparticle formation by plant leaf extract (Aisida et al., 2019).

Table 1. was represented many researchers' works that summarize the green synthesis of Ag NPs including the name of the plant used, morphology/size of Ag NPs, and type of application.

Table 1. Comparative study of the biosynthesized Ag NPs using various plant extracts

No.	Plant	Morphology/ size (nm)	Application	Reference
1	*Galinsoga Parviflora*	20	Antibacterial and Antioxidant Activities	(Thangavelu et al., 2018)
2	*Chenopodium murale*	30 & 50	Antioxidant and antibacterial activity	(Abdel-aziz et al., 2013)
3	*Thymus vulgaris*	40	Antibacterial activity	(Paula et al., 2020)
4	*Cestrum nocturnum*	20	Antioxidant and antibacterial	(Kumar et al., 2020)
5	*Erythrina suberosa (Roxb.)*	50	Antimicrobial, antioxidant, and cytotoxic	(Mohanta et al., 2017)

2.4. Description of *Foeniculum Vulgare* Plant

2.4.1. Chemistry of *Foeniculum vulgare*

Fennel is the common name for *Foeniculum vulgare*. It is a very aromatic annual, biennial medicinal, or branched perennial herb that grows in a variety of climates around the world. *Foeniculum vulgare* is a perennial herb having therapeutic properties that belong to the *Umbelliferae family (Apiaceae)* (Beyazen et al., 2017). It is hardy, with feathery leaves and hair-like foliage, and grows to a height of up to 2.5 meters tall with hollow stems, and branches well. The fruit is a dry, grooved seed that ranges in length from 4 to 10 mm, weighs 6 to 7 mg, and is elliptical and slightly curved (Cabral et al., 2017). The leaves can grow up to 40 cm long and are finely divided, with filiform (threadlike) final segments around 0.5mm wide. Leaves are 3-4 pinnate, filiform, and up to 4 cm long; leaf bases are sheathed. It features a green, smooth, and slippery stem with tall stiff branches and linear segments of many divided leaves. Small yellow or brilliant golden flowers grow in big flat-topped umbels. In most areas, it grows wild. Fennel is an ancient spice plant that widely grows in arid and semi-arid climates

(Badgujar et al., 2014). The detailed taxonomy is shown in table 1. It was native to southern Europe and the Mediterranean region. *Foeniculum vulgare* has been reported to contain 6.3% of moisture, 9.5% protein, 10% fat, 13.4% minerals, 18.5% fiber, and 42.3% carbohydrates. The minerals and vitamins present in the *Foeniculum vulgare* are calcium, potassium, sodium, iron, phosphorus, thiamine, riboflavin, niacin, and vitamin C (Rather et al., 2016).

It is now commonly grown in temperate and tropical climates around the world. The genus name *Foeniculum* (Latin for little hay) probably refers to the aroma of fennel and is the source of the name of fennel in many contemporary European languages. *Foeniculum vulgare* is a highly aromatic and flavourful herb with medicinal application (Rani, 2016). *Foeniculum vulgare* mill, also known as "ensilal," grows in Ethiopia's grassland areas. The plant is mostly found in northern Ethiopia (Dessie, Komolcha, and Hayek), eastern Ethiopia (near Harar, Jigjiga), and southern Ethiopia. The herb is chewed with chat in Ethiopia and used to treat kidney stones and gonorrhea (Rasul et al., 2012). In addition, the plant was used to flavor "caticala," "local areke," and "tej" in the Dessie area. Fever, flatulence, gastralgia, kidney, gastritis, sleeplessness, renal problems, laxative, leucorrhoea, diuretic, nosebleed, diaphoretic, liver discomfort, mouth ulcer, and stomachache are all treated with this herb (Endalamaw & Chandravanshi, 2015). Moreover, this plant has been investigated extensively for several medicinal and therapeutic activities and has been reported for possessing carminative, flavoring, antioxidant, antibacterial, antifungal, and mosquito repellent properties (Esquivel-Ferriño et al., 2012).

Figure 4. Leaf of *Foeniculum vulgare* (Badgujar et al., 2014).

Terpenoids, flavones, tannins, glycosides, saponins, phenols, alkaloids, and other types of compounds are phytochemicals present in the *Foeniculum vulgare*. The characteristic anise odor of *Foeniculum vulgare* which is due to its essential oil makes it an excellent flavoring agent in baked goods, meat and fish dishes, ice cream, and alcoholic beverages. The major components of *Foeniculum Vulgare* leaf essential oil have been reported to be α-phellandrene (11%) (**1**), fenchone (10.8%) (**2**), estragol (10.1%) (**3**), and trans-anethole (47%) (**4**) with their chemical structures (Mehra, Tamta, & Nand, 2021) shown in Figure 4.

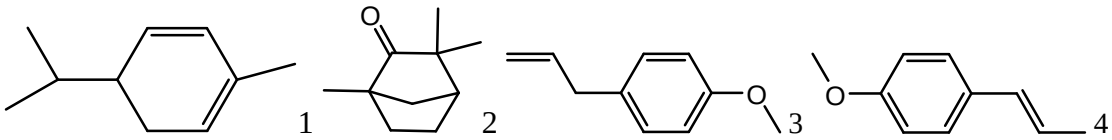

Figure 5. Molecular structures of the major bioactive essential oil of *Foeniculum Vulgare* (Rather et al., 2016).

2.4.2. *Foeniculum vulgare* for silver nanoparticles synthesis

In *Foeniculum vulgare* extracts, enol- to keto-transformation is the key factor in the synthesis of biogenic Ag NPs (Singh P. et al., 2016). *Foeniculum vulgare* leaf extracts contained secondary metabolites which act as antimicrobial agents. The functional groups found in the *Foeniculum vulgare* leaf plant (such as –C–O–C–, –C–O–, –C=C–, and –C=O–) are present in phytochemicals such as flavones, alkaloids, phenols, and anthracenes can help to produce Ag NPs. These functional groups are acting as the capping ligands of the Ag NPs confirmed by FT-IR analysis. The main function of the capping ligands is to stabilize the Ag NPs to control further growth and agglomeration. *Foeniculum vulgare* leaf contains polyphenols and phenolic acids, such as 3-O-caffeoylquinic acid, 4-O-caffeoylquinic acid, 5-O-caffeoylquinic acid, 1, 3-O-di-caffeoylquinic acid, 1, 4-O-dicaffeoylquinic acid, and 1, 5-O-di-caffeoylquinic acid among the major bio-components, which have antibacterial activity, and several different useful properties (Dessie et al., 2020).

2.4.3. Antimicrobial activity of *Foeniculum vulgare*

Secondary metabolites found in medicinal plants include alkaloids, glycosides, saponins, flavonoids, and tannins, which are generally superior in antimicrobial activity. Many bacterial, fungal, viral, and mycobacterial infectious illnesses are treated with fennel. It has antimicrobial activity due to compounds such as undecanal, 1, 3-benzenediol, oleic acid, and 2, 4-undecadienal (Mehra, Tamta, Nand, et al., 2021). *Foeniculum vulgare* shows anti-microbial activity in a wide variety of microorganisms. Antibacterial activity of the *Foeniculum vulgare* leaf was evaluated against *Escherichia coli, Staphylococcus aureus, Listeria monocytogenes, Bacillus pumilus,* and *Enteropathogenic E. coli* (EPEC). Fennel's extract exhibits maximum antibacterial activity against *Staphylococcus aureus* showing 20.00 mm of inhibition zone (Al-Hadid, 2017).

2.4.4. Antioxidant activity of *Foeniculum vulgare*

Foeniculum vulgare was known as an excellent source of natural antioxidants and contributed to the daily antioxidant diet and it was found to exhibit a free radical scavenging activity with higher content of phenolic and flavonoids and showed the highest DPPH scavenging activity (Shahat et al., 2011). Phenolic compounds of *Foeniculum vulgare*, was including caffeoylquinic acid, rosmarinic acid, eriodictyol-7-orutinoside, quercetin-3-O-galactoside, and kaempferol-3- O-glucoside, these compounds showed antioxidant activities. The volatile oil showed strong antioxidant activity in comparison with butyrated hydroxyanisole and butylated hydroxytoluene (Badgujar et al., 2014). Therefore, *Foeniculum vulgare* extract can play a dual role as an antioxidant and antibacterial agent and has good potential to be applied in the food and pharmaceutical industry. In addition, *Foeniculum vulgare* showing antioxidant activity might be explored for functional food and nutraceutical applications, besides its traditional uses.

2.5. Characterization of Silver Nanoparticles

Characterization of Ag NPs is important in determining phase purity, shape, size, morphology, structure, and surface charge, among other things, by utilizing advanced analytical techniques such as XRD, UV-vis spectroscopy, FT-IR, SEM, and so on (Sivakumar et al., 2018).

2.5.1. X-ray diffraction spectroscopy (XRD)

XRD is used to analyze crystal structures, qualitatively identify various compounds, quantitatively resolve chemical species, and measure crystallinity, and particle sizes of Ag NPs (Quinn & Benzonelli, 2018). When X-ray light reflects on a crystal, many diffraction patterns form and the patterns reflect the physicochemical properties of the crystal structures. In a powder specimen, diffracted beams typically come from the sample and reflect its structural physicochemical features (Ali et al., 2014). Analysis of these materials largely depends on the formation of diffraction patterns. Each material has a unique diffraction beam which can define and identify it by comparing the diffracted beams with the reference database in the Joint Committee on Powder Diffraction Standards (JCPDS) library. Therefore, XRD has long been used to define and identify bulk and nanomaterials, forensic specimens, and industrial, and geochemical sample materials (Kgatshe et al., 2019). The use of XRD measurement has the advantage of allowing the material to be analyzed without causing damage to it. The Scherrer equation uses to describe the working of XRD: -

$$D \approx \frac{\kappa\lambda}{\beta cos\theta} \qquad (4)$$

Where D is the crystal size/particle size (nm), K is the Scherrer constant, λ is the wavelength of X-ray, θ is the Braggs angle in radians and β is the full width at half the maximum (FWHM) of the peak in radians (Rajeshkumar & Bharath, 2017).

The dislocation densities of synthesized nanoparticles are calculated using

$$\delta = \frac{1}{D^2} \qquad (5)$$

Where δ is the density of dislocations and D is the crystalline size.

2.5.2. UV-Visible spectroscopy

UV-vis spectroscopy is a very useful method for characterizing synthesized nanoparticles, and it is used to monitor the stability of Ag NPs. Ag NPs have unique optical properties that allow them to interact strongly with specific wavelengths of light (Begum et al., 2018). Furthermore, UV-vis spectroscopy is quick, simple, selective for different types of nanoparticles, requires only a short measurement time, and no calibration is required for particle characterization of colloidal suspensions (Tomaszewska, Soliwoda, Kadziola, Tkacz-szczesna, et al., 2013). The conduction band and valence band in Ag NPs are very close to each other, allowing electrons to move freely. These free electrons cause a surface Plasmon resonance (SPR) absorption band to form as a result of the collective oscillation of electrons in resonance with the light wave. The absorption of Ag NPs depends on the particle size, dielectric medium, and chemical environment. The maximum absorption of Ag NPs has been reported to 0.7, and Plasmon resonance produces a peak near 400 nm, confirming the synthesis of Ag NPs (Tomaszewska, Soliwoda, Kadziola, Tkacz-Szczesna, et al., 2013).

The Tauc relations are used to calculate the energy bandgap for the samples (Jubu et al., 2020):-

$$(\alpha h\nu)^2 = \kappa(h\nu - Eg) \qquad (6)$$

Where α absorbance co-efficient, h is Plank constant, ν is incidental UV radiation frequency, κ is Constant, hν is Energy, and Eg is Band gap energy.

$$Eg = \frac{1240}{\lambda_{max}}(eV) \qquad (7)$$

Absorbance co-efficient α is calculated as

$$\alpha = 2.303 \times \frac{A}{t} \qquad (8)$$

Where A is absorbance and t is the thickness of the cuvette. As a result, its value is 1 cm.

The absorption coefficient measures the amount of light that might be absorbed by a given sample thickness; it tells us how much light at a specific wavelength will be absorbed by materials (Jubu et al., 2020).

2.5.3. Scanning electron microscopy (SEM)

SEM is a type of electron microscope that produces images of a sample by scanning the surface with a focused beam of electrons. Among different electron microscopy techniques, SEM is a surface imaging method, used to characterize different nanomaterial shapes, and the surface morphology of the synthesized particles at the nanoscales. The modern high-resolution SEM can identify the morphology of nanoparticles below the level of 10 nm (Fissan et al., 2014). Electrons interact with atoms in the sample, producing a variety of signals that contain information about the surface topography and composition of the sample. SEM images showed that most of the Ag NPs are predominately spherical having a smooth surface and well dispersed with a close compact arrangement (Khan et al., 2018)

2.5.4. Fourier transform infrared (FTIR) spectroscopy

FT-IR technique is one of the most potent tools for determining chemical bond types (functional groups) and structural features in the plant's biomolecules that are responsible for the reduction and stabilization of the silver ion. For FT-IR analysis, synthesized Ag NPs and plant extract could be in the solid or liquid state. FT-IR spectroscopy is frequently used to find out whether biomolecules are involved in the synthesis of nanoparticles, which is more pronounced in academic and industrial research (Lin et al., 2014).

2.6. Antimicrobial and Antioxidant Activities of the Biosynthesized Silver Nanoparticles

2.6.1. Antibacterial and antifungal activity of synthesized silver nanoparticles

Nanosilver is called a killing agent due to its potential to kill Gram-positive and Gram-negative bacteria as well as antibiotic-resistance strains very effectively. Ag NPs can bind with the bacterial cell wall and plasma membrane (Dakal et al., 2016). The function of the cell wall and

membrane is to preserve the microorganism against environmental injury. Bacterial classification is based on the differences in cell wall structures; a Gram-negative cell wall, called a cell envelope, contains at least two layers of lipopolysaccharides whereas a Gram-positive cell wall is typically thicker and primarily composed of a single type of molecule, peptidoglycans.

Ag NPs have higher antibacterial activity against Gram-positive bacteria than Gram-negative bacteria, due to the peptidoglycan layer, made of glycan strands cross-linked by short peptides and anionic glycopolymers called teichoic acid, in the Gram-positive bacterial cell wall provides a natural barrier that prevents penetration of the nanoparticles. On the other hand, Gram-negative bacteria have a thinner cell wall and less peptidoglycan. The well-defined antibacterial activity of Ag NPs has the capability of destroying the structure within the cell, producing reactive oxygen species and free radicals that stimulate cellular toxicity and oxidative stress, and regulate the signal transduction pathway. When microorganisms are served with Ag NPs, Ag NPs bind to the cell wall of the pathogen and cause the shrinkage of the cytoplasm and busting of the cell wall (Durán et al., 2016). Gram-negative bacteria are the bacteria that retain the color of the stain even after washing with alcohol or acetone and include genera such as *Escherichia coli,* and *Pseudomonas aeuruginosa*. Gram-positive bacteria are the bacteria that lose the color of the stain after washing with alcohol or acetone and include many well-known genera such as *Bacillus subtilis,* and *Staphylococcus aureus* (Anbu et al., 2019).

Pathogenic fungi are those fungi that cause disease in animals and humans. Those are considered to play a vital role in causing fungal infections, especially in hospitals. Although fungi are eukaryotic organisms, on the other hand, many pathogenic fungi are also microorganisms. The study of pathogenic fungi is referred to as *Mycology* (Saravanan et al., 2018). Along with the antibacterial activities of the Ag NPs, numerous studies had been reported on the antifungal efficacy of Ag NPs, which reveal that silver nanoparticles could be used as an effective antifungal agent because Ag NPs exhibit excellent antifungal characteristics against several fungal species. In a study, the antifungal activities of the Ag NPs against different fungal strains such as *Trichophyton mentagrophytes* and *Candida albicans* fungi and observed, and Ag NPs exhibited good antifungal activity. Later, the antifungal

activity of the Ag NPs fabricated by the modified Tollens process was evaluated for common pathogenic *Candida sp*. in terms of the determination of the minimum inhibitory concentration (MIC), minimum fungicidal concentration (MFC), and the time-dependency of yeasts growth inhibition reported by the silver NPs effectively inhibited the growth of the tested yeasts at the concentrations below their cytotoxic limit against the tested human fibroblasts determined at a concentration equal to 30 mg/L of Ag NPs (Zodrow et al., 2009). Moreover, compared with bacteria, fungi have higher tolerances too, and uptake competencies for, metals, particularly in terms of the high wall-binding capability of metal salts with fungal biomass for the high-yield production of nanoparticles (A. E. Mohammed, 2015). Nanosilver is a more effective and fast-acting fungicide against a broad spectrum of common fungi including genera such as *Candida Albicans* (Mallmann et al., 2015).

2.6.2. Antioxidant activity of synthesized silver nanoparticles

Keshari *et al*., tested the leaf extracts of the medicinal plant, *Cestrum nocturnum* for Ag NPs production and antioxidant activity studies. He observed that 16 µg/mL of green synthesized Ag NPs showed maximum (29.55%) radical scavenging activity. The plant phenolic compounds are responsible for the conversion of silver nitrate into Ag NPs and exhibit antioxidant activity (Keshari et al., 2020). Mohammed *et al*., produced Ag NPs using *Moringa oleifera* plants, and these particles showed antioxidant activity against DPPH reagent. The antioxidant activity of Ag NPs was assayed using 2, 2-diphenyl-1- picrylhydrazyl (DPPH) to determine the scavenging function of free radicals. In this assay, the removal of the H-atom from the antioxidant compound leads to reducing the color of DPPH from violet to a pale yellow. The higher scavenging activity of free radicals was related to more decrease in absorbance, which was calculated using the following formula:

$$\text{DPPH scavenging activity (\%)} = \frac{100 \times (A_0 - A_1)}{A_0}$$

Where A_0 is the absorbances of the control and A_1 is the sample absorbances (Mohammed et al., 2022). Similarly, Saygi *et al*., used the flower extracts of *Tilia cordata* plants for biosynthesis of Ag NPs than applied for radical scavenging activity (Saygi & Cacan, 2021).

2.7. Other applications of Silver Nanoparticles

Silver nanoparticles have an important role in making desirable materials for different industries. Silver nanoparticles with a diameter of 100 nm are very important for large-scale industries due to their small particle size, high surface area, quantum confinement, and spread without agglomeration. Silver nanoparticles hold numerous applications including catalytic, electrical, food storage, sanitization system, deodorants, socks, and textile coatings. Furthermore, silver nanoparticles have many important uses, including spectrally sensitive solar energy absorption coatings and intercalation content for electrical batteries, optical receptors, polarizing filters, chemical reaction catalysts, bio-labeling, and antimicrobial agents. In the agricultural sector, silver nanoparticles apply to control the food security challenges raised by climate change. Currently, silver is used in the expanding field of nanotechnology and appears in many consumer products. Silver nanoparticles synthesized through the green method have many biomedical applications as well as in controlling pathogenic microbes (Modi, 2018).

3. MATERIALS AND METHODS

3.1. Description of Study Area

The leaf of *Foeniculum vulgare* was collected from the southern part of Ethiopia, Sidama regional state, Wondo Genet zone located at 219 km far from Adama city. The sample preparation, leaf of *Foeniculum vulgare* extraction, biosynthesis of silver nanoparticles, antioxidant activity, characterization using (XRD) and Scanning Electron Microscopy (SEM) were done in the Laboratory of Adama Science and Technology University (in the schools of Applied Chemistry, Materials Science Engineering, and Applied Biology respectively), evaluation of antibacterial activity test was done in Adama Science and Technology University in the Applied Biology Laboratory. UV-Vis spectroscopy and Fourier Transform Infrared (FTIR) characterization were done at Bahir Dar University. The antifungal activity test was performed at Haramaya University in the Biology Laboratory.

3.2. Chemicals and Instruments

3.2.1. Chemicals and reagents used

The chemicals and reagents required for the preparation of silver nanoparticles and the phytochemical analysis were silver nitrates ($AgNO_3$ 99.9%, AR analytical reagent, Trust Chemicals), distilled water, Sodium hydroxide (NaOH 99%, Sigma aldrich), Ferric chloride ($FeCl_3$ 99%, Sigma aldrich), Ethanol (C_2H_5OH 99.8%, Fmd, Ethiopia), Methanol (CH_3OH 99.8%, Loba Chemie), Hydrochloric acid (HCl, Riedel dehaen, Germany, 37% HCl), Sulfuric acid (H_2SO_4 98%, Sigma aldria), Iodine (I 98.5%, Loba Chemie) Potassium iodide (KI 99.8%, Samir tech-chem), Chloroform ($CHCl_3$ 99.8%, Blulux), Benedict's solution, Ascorbic acid (98%, Sigma Aldrich), 2, 2-dipphenyl-1 picrylhydrazyl (DPPH 97%, Sigma Aldrich), Dimethyl sulfoxide (DMSO 99.5%, SRL), Mueller Hinton Agar (Alpha Chemika), Potato Dextrose Agar (Alpha Chemika), Sabouraud Dextrose Agar (Alpha Chemika), and the leaf of *Foeniculum vulgare* medicinal plant were chemicals used in this research work. Solvents and chemicals were purchased from commercially available suppliers (Fine chemical and

Firmament chemical supplier, Addis Abeba) and all those chemicals were used without any further purification.

3.2.2. Apparatus and instruments

Pipette, aluminum foil, spatula, test-tube with a test-tube rack, brown bottle, electronic beam balance, electrical grinding machine, vials, beaker (800 mL, 500 mL, and 100 mL), magnetic stirrer with hot plate, bare magnet, petri-dish, conical flasks (500 mL and 100 mL), volumetric flasks (500 mL and 100 mL), funnels, measuring cylinders (100 mL and 50 mL), Erlenmeyer flask, oven, Whatman filter paper to filter the extract, refrigerator, ceramic crucible, mortar and pestle, dropper, centrifuge (LC-04C) were apparatuses and instruments to be used for this study. The laboratory instruments that were used for characterizing the biosynthesized silver nanoparticles were mentioned as follows: X-Ray Diffraction (XRD-7000, Shimadzu Co., Japan) was used to characterize the nature of the crystal structure of the biosynthesized silver nanoparticles. UV-Vis spectroscopy (V-770, Dual-beam UV-VIS spectrometer, Azzota corp., USA) was used to study the optical properties of the biosynthesized silver nanoparticles, and Fourier Transform Infrared (FT/IR-6600typeA, JASCO) was used to characterize the presence of functional groups of the biosynthesized silver nanoparticles, and Scanning Electron Microscopy (SEM, JEOL, JCM-6000Plus, Japan) was used to study the composition, texture, and morphology of the prepared silver nanoparticles.

3.3. *Foeniculum Vulgare* Leaf Collection and Extract Method

3.3.1. Collection of *Foeniculum Vulgare* leaf

Foeniculum vulgare leaf was collected from the agricultural plots of Wondo Genet Agricultural Research Centre, in Sidama Region, Ethiopia. The leaf samples were washed several times with distilled water to remove extraneous matter, impurities, and dust particles. The cleaned leaf was completely dried at room temperature in the open air and under shadow for about two weeks (15 days) to remove any remaining moisture content from the leaf. The dried leaf was chopped and crushed by using an electrical grinding machine to produce a fine powder followed by packing in a brown bottle by covering the whole body of the bottle with aluminum foil to protect against the effect of light.

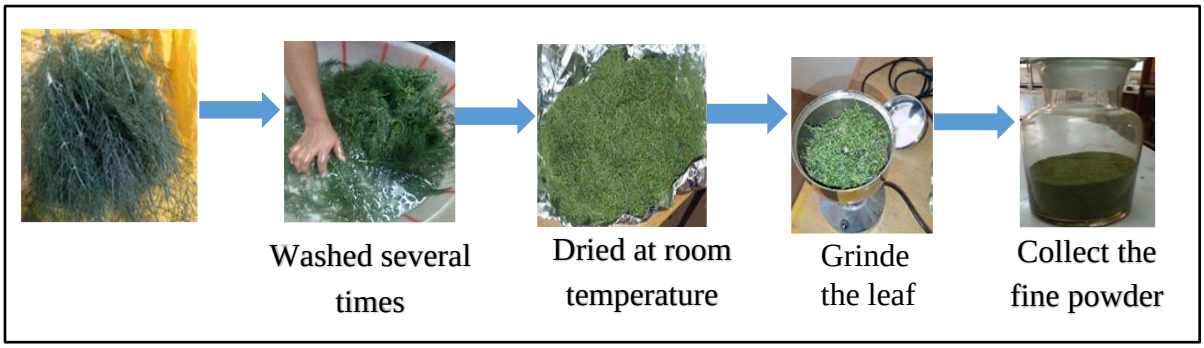

Figure 6. The general process of collection and sample preparation of *Foeniculum vulgare* leaf.

3.3.2. Preparation of *Foeniculum vulgare* leaf extract

The preparation of *Foeniculum vulgare* Leaf extract was carried out using a modified procedure reported by Gudimalla *et al.*, (Gudimalla, Jose, Rajendran, et al., 2021). The extraction was carried out by taking 25 g of the powdered leaf of *Foeniculum vulgare* in 800 mL of the glass beaker containing 500 mL of distilled water. The beaker was covered with aluminum foil, to prevent the effect of light. After that, the mixture was stirred using a magnetic stirrer for 15 min and allowed to be heated at 50 °C for 1 hour on a magnetic stirrer with a hot plate, after 1 hour the heater was turned off and the mixture was allowed to cool down to room temperature and settle as shown in Figure 7. After settlement, the prepared extract was filtered twice with Whatman No. 1 filter paper to get a clear solution for further experiments. Finally, the filtrate was stored within a refrigerator at 4 °C for Ag NPs synthesis (Gudimalla, Jose, Rajendran, et al., 2021).

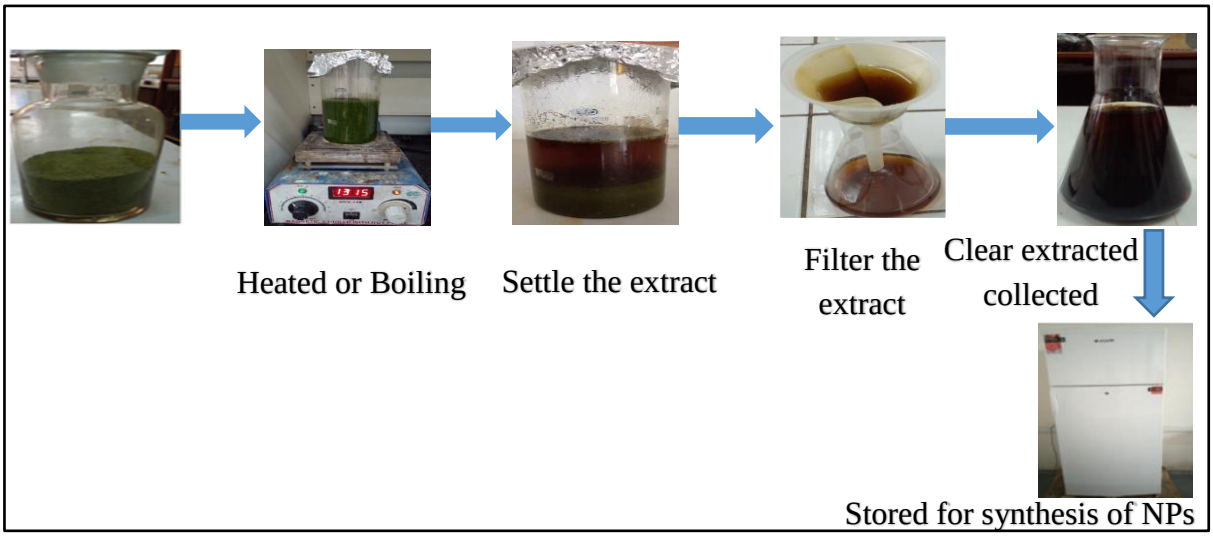

Figure 7. Preparation of *Foeniculum vulgare* leaf extract.

3.4. Phytochemical Test of *Foeniculum vulgare* Leaf Extracts

Foeniculum vulgare leaf extract was used as a reducing agent and capping agent, it was necessary to assess whether the phytochemicals, such as flavonoids, phenols, alkaloids, etc, do naturally exist in the extract or not. A phytochemical test was used to detect the presence of alkaloids, flavonoids, saponins, steroids, tannins, and terpenoids were carried out using standard methods.

Test for Alkaloids (Wagner's test)

The presence of alkaloids in leaf extract checked through Wagner's test by using the aqueous leaf extracts of 2 mL solution were dissolved in Wagner's reagent (Iodine in Potassium Iodide) in the test tube (Nisha & Suja, 2018).

Test for Flavonoids

The presence of flavonoids in the leaf extract was checked through an alkaline reagent test by using 5 mL of aqueous leaf extract treated with a three drops of sodium hydroxide solution (NaOH) (Garg et al., 2019).

Test for Tannins (Ferric Chloride Test)

5 mL of aqueous leaf extract was dissolved in 5 mL of distilled water and three drops of 1% ferric chloride solution were added to confirm the presence of tannins (Shaikh & Patil, 2020).

Test for Terpenoids (Salkowski test)

The presence of terpenoids in the leaf extract was checked through chloroform by using 4 mL of extract followed by the addition of 3 mL of chloroform. Then, 3 mL of concentrated sulfuric acid (H_2SO_4) was carefully added to form a layer (Cp, 2017).

Test for Steroids

The presence of steroids in leaf extract was checked through salkowski test by using 2 mL of chloroform and concentrated H_2SO_4 was added with the 5 mL aqueous plant crude extract (Yaseen et al., 2017).

Test for Glycoside

The presence of glycoside in leaf extract was checked through salkowski test by using 2 mL of concentrated H_2SO_4 added to the aqueous plant extract (Nisha & Suja, 2018).

Test for Benedict

The presence of reducing sugar in the leaf extract was checked through the benedict test by using 3 mL of aqueous leaf extract was taken into a test tube then benedict reagent was added drop by drop and heated for 2 min (Egbuna et al., 2019).

Test for Phenols

The presence of the phenolic functional group in leaf extract was checked by using 5 mL of aqueous extract taken into a test tube and 5 drop of 3% of $FeCl_3$ was added in to an extract drop by drop wisely (Yaseen et al., 2017).

Test for Saponins

The presence of saponins in leaf extract was checked through a frothing test by using 3 mL of aqueous plant extract dissolved in 5 mL of distilled water and the mixture was shaken vigorously (Bano & Deora, 2019).

3.5. Green Synthesis of Silver Nanoparticles

The biosynthesis of Ag NPs has been carried out by adapting the reported procedure by Desalegn *et al*. (Desalegn et al., 2020), with minor modifications. Silver nitrate was used as a precursor for the biosynthesis of silver nanoparticles using *Foeniculum vulgare* leaf extracts.

Silver nanoparticles were biosynthesized in three different volume ratios using *Foeniculum vulgare* leaf extract 1:1 (100:100), 1:3 (50:150), and 3:1(150:50) by using 0.1 M of the silver nitrate salt precursor respectively in a separate beaker. A small-sized magnetic bar was put inside the beaker containing the leaf extract and the precursor solution to enhance the reaction kinetics. Then the mixtures were heated at 30 ^{0}C for 1 h on the hot plate with stirring and after 1 h, the heater was turned off and the mixtures were stirred for 3 h without heating. The mixtures were heated to from a brownish color which indicates the formation of its silver nanoparticles. Then, after the stirring reaction time was completed the formed silver nanoparticles at different volume ratios were allowed to stay within a refrigerator overnight to cool down and settled. Then the mixture above was decanted and the formed precipitate for each of the individual ratios was washed with ethanol and distilled water 3 times followed by centrifugation for 15 min at 15000 rpm. After the end of the centrifugation, the formed silver nanoparticles for each of the individual ratios were collected using a crucible ceramic dish and placed into a drying oven at 100 °C. After drying, it was allowed to cool and the obtained product was ground into small fine powder by a mortal. Finally, the gray powder of silver nanoparticles was obtained. At last, the powder of silver nanoparticles was put in the sample holder and packed for the next characterization methods and for examined its antimicrobial and antioxidant activities. The whole procedure has been summarized in Figure 8.

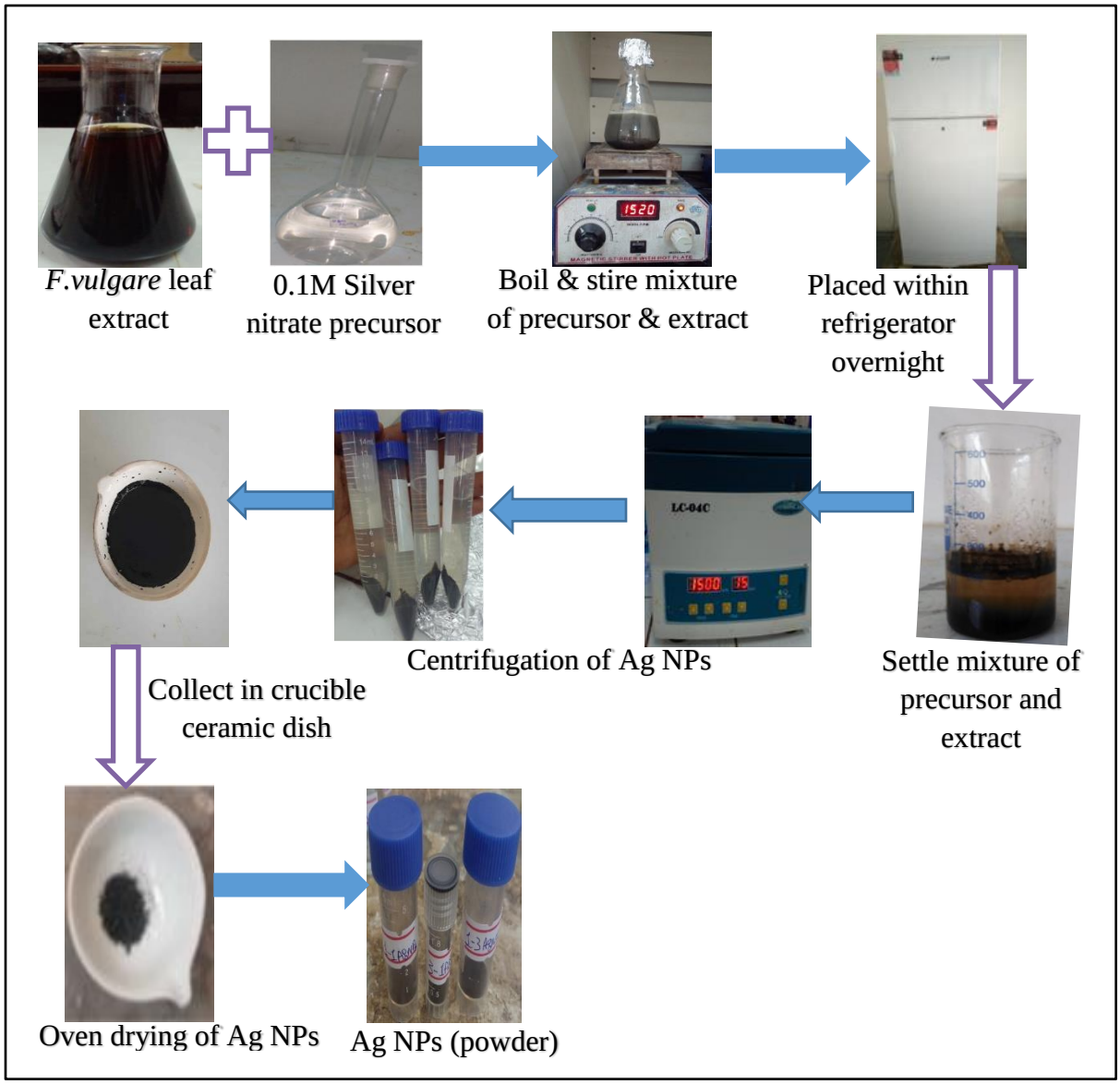

Figure 8. Biosynthesis process of silver nanoparticles.

3.6. Characterization Techniques of the Biosynthesized Silver Nanoparticles

The biosynthesized silver nanoparticles were characterized for the crystallite size, optical properties, surface morphology, and functional group by using analytical tools such as X-Ray diffraction (XRD), Ultra-violate visible spectrophotometer (UV-Vis), Scanning Electron Microscopy (SEM), and Fourier Transform Infrared (FTIR) Analysis, respectively.

3.6.1. X-ray diffraction analysis

The crystalline structure/amorphous nature, the average crystallite size and lattice structure of a crystalline substance of the biosynthesized Ag NPs were identified by using the XRD diffractometer (Shimadzu-radiation operates at a voltage of 40 kV and applied current of 30 mA with Cu Ka radiation, λ=1.541 Å) and the collected data were scanned & recorded in the range of 2θ from 10 to 80 (Gudimalla, Jose, Varghese, et al., 2021).

Sample preparation: 1.5-2.5 grams of dried Ag NPs were ground by mortar and pestel and then it was filled into the sample holder and subjected to an X-ray diffractometer.

3.6.2. UV-Visible absorbance spectroscopic analysis

UV-Visible spectra were carried out using spectrophotometry for monitoring the biosynthesis of Ag NPs. UV-Vis absorption spectral analysis was used to evaluate the optical properties of the biosynthesized Ag NPs and measured by using a UV-visible spectrophotometer. A spectrum was recorded from a wavelength of 200 nm to 800 nm against an absorbance, with a resolution of 1 nm (Lakshmi et al., 2013).

Sample preparation: Finely ground powder of Ag NPs dissolve by DMSO then packed into a Uv-Vis sample holder then the holder was placed in Uv-Vis spectrophotometer and absorbance was recorded.

3.6.3. Fourier transform infrared (FTIR) analysis

FTIR analysis was used for determining the presence of potential biomolecules, chemical composition, and functional groups of the biosynthesized Ag NPs. The different peaks in the IR spectrum were interpreted for the different functional groups in the formulations and the main information obtained from FT-IR was recorded (Z. A. Ali et al., 2016).

Sample preparation: The biosynthesized Ag NPs powders of the nanomaterial were mixed with potassium bromide (KBr) and diluted to form a very fine powder. The powder was then compressed into a thin transparent pellet which was used for recording the FTIR spectrum. The procedure is the same for *Foeniculum vulgare* leaf powder.

3.6.4. Scanning electron microscopy analysis

SEM analysis was used to study morphology, structural features, micrograph images, and size of the biosynthesized silver nanoparticles. This characterization was shown agglomerations of individual silver nanoparticles (Gudimalla, Jose, Varghese, et al., 2021).

Sample preparation: Small amount of Ag NPs silver nanoparticles powder sample was dispersed in acetone and sonicated for a few minutes. Some samples need to be coated to make them conductive. Metals require no preparation due to their inherent ability to conduct electricity. However, non-metals need to be coated with a conductive material such as gold/ gold-palladium alloy, using a sputter coater.

3.7. Method of Antimicrobial Evaluation

The bacteria and fungi are used for inhibitory zone tests to investigate the antimicrobial properties of silver nanoparticles using the agar well method. The antimicrobial studies were evaluated and carried out on four bacterial strains*;* two Gram-negative *(Escherichia coli,* and *Pseudomonas aeruginous),* and two Gram-positive *(Staphylococcus aureus, and Streptococcus Pyogenes)* which were obtained from the Applied Biology Department laboratory of Adama Science and Technology University and two fungal strain; *Aspergillus niger* and *Candida albicans* were performed in Haramaya University.

3.7.1. Method of antibacterial activity test

The biosynthesized silver nanoparticles (1:1, 1:3, and 3:1 ratio) were screened for in-vitro antibacterial activities against four bacteria strains; two Gram-negatives (*E.coli and P. aeruginosa*), and two Gram-positive (*S. aureus* and *S. Pyogenes*) by Agar disc diffusion method. The medium was prepared by dissolving 38 g of Mueller Hinton Agar medium in 1000 mL of distilled water and autoclaved at 121 °C for 15 min. The autoclaved medium was poured into sterile plates (20-25 mL/plate) and the plates were allowed to solidify under the sterile condition at room temperature. After solidification, the plates were seeded with overnight grown culture approximately 1.5 X 10^8 CFU/mL (McFarland standard) by swabbing evenly onto the surface of the medium with a sterile cotton swab.

Then, 35 mg from each of the three ratios of Ag NPs (1:1, 1:3, and 3:1) at the concentrations of 50 μg/mL, 75 μg/mL, and 100 μg/mL per disc was prepared by dissolving within 1 mL of DMSO and stirred using a magnetic stirrer for 30 min. From this solution about different concentrations (50 μg/mL, 75 μg/mL, and, 100 μg/mL) were poured using a micro pipette in each pathogen well. Whatmans filter paper no. 1 was used to prepare discs approximately 6 mm in diameter. From each different ratio, 80 μL was taken and saturated with discs (6 mm diameter) and positioned on the surface of the medium with sterile forceps and gently pressed down to ensure contact with the MHA. Control experiments were carried out under similar conditions using amoxicillin for antibacterial activity as a standard drug. The plates were inverted and then incubated at 37 °C for 24 h. After incubation, the inhibition zone produced by Ag NPs were evaluated by measuring the diameter (mm) of the clear zone around the disc against the test organisms using a ruler and reporting the result. The antibacterial activities of biosynthesized Ag NPs were done in collaboration with the Department of Applied Biology, Adama Science and Technology University.

3.7.2. Method of antifungal activity test

The solutions (15, 20, and 25 mg/mL) of Ag NPs were prepared by reconstituting 0.015, 0.020, and 0.025 gm of each of the Ag NPs powder in 10 mL of DMSO. For preparing the 15 mg/mL, 20 mg/mL, and 25 mg/mL solutions of the Ag NPs were transferred to separate 10 mL capacity volumetric flasks (Alabi & Huisman, 2012). Antifungal activities of Ag NPs (1: 1, 1: 3, and 3: 1 ratio) against *Aspergillus niger* and *Candida albicans* were similarly determined using the disc diffusion method. First PDA and SDA were prepared by dissolving the required amount of PDA and SDA powders with distilled water. Then the mixture was heated on the hot plate and autoclaved to get a boiled and uniform solution. The resulting autoclaved medium was transferred into separate petri plates and allowed to solidify. Within 15 min of adjusting the turbidity of the suspension of inoculums, a sterile cotton swab was dipped into the adjusted suspension and rotated several times by pressing firmly on the inside wall of the tube above the fluid level. This removes excess fluid from the swab. Then, the dried surface of PDA and SDA plates was inoculated by streaking using the swab three times over the entire surface by rotating the PDA and SDA plates at approximately 60° each time to ensure an even distribution of the inoculums. Then, the PDA and SDA plates were left open in the hood for three to five

minutes to allow for any excess surface moisture to be absorbed (CLSI, 2012). For the application of the Ag NPs, discs of 6 mm diameter were prepared from sterile filter paper cut into small, circular pieces of equal size by a perforator and then they were impregnated each with 0.01 mL of the prepared test silver nanoparticles.

The Ag NPs-impregnated discs were placed onto the surface of the inoculated agar plates using sterile forceps. Each disc was pressed down to ensure complete contact with the agar surface. The discs were distributed evenly so that they were no closer than 24 mm from center to center (CLSI, 2012). Discs of commercial Ketoconazoale/Tilt (10 units/disc) were used as positive controls while DMSO-impregnated discs were used as negative controls. Then the PDA and SDA plates were sealed with Parafilm and incubated at 27 °C for 5 to 7 days for fungal pathogens. After incubation, the diameters of the zone of inhibition around each disc were measured to the nearest millimeter along two axes (i.e. 90° to each other) using a transparent ruler and the means of the two readings were recorded. For each selected pathogen the experiment was carried out with three replications (Bengal, 2013; Thompson & Lowe, 2011). The zone of inhibition was measure and represented as Mean ± SD. The antifungal activities of biosynthesized Ag NPs were done in collaboration with the Department of Biology, Haromaya University.

3.8. Method of Antioxidant Activity Test

DPPH radical-scavenging assay (RSA): The DPPH assay was used to assess the free radical scavenging activity of the biosynthesized Ag NPs (1:1, 1:3, and 3:1 ratio) within three different volumes of ratios. The free radical scavenging activity of the biosynthesized Ag NPs were measured by the 2, 2-diphenyl-1-picryl-hydrazyl (DPPH) method (Foti, 2015). With this method, it is possible to determine the radical scavenging power of an antioxidant by measuring the decrease in the absorbance of DPPH at 517 nm.

The stock solution was prepared by taking 8 mg of Ag NPs and adding to 5 mL of methanol to dissolve it. The serial solution was done to give 50, 100, 200, 400, and 800 µg/mL in five vials. The 1 ml of each biosynthesized Ag NPs at various concentrations (50, 100, 200, 400, and 800 µg/ml), 4 mL DPPH (prepared in methanol by dissolving 4 mg DPPH in 100 mL methanol)

was added then the mixture was shaken vigorously and the resulting solution was placed in dark place at 37 °C for 30 minutes and subjected to a UV-Vis spectrophotometer to record absorbance at 517 nm. Ascorbic acid was used as a reference standard and dissolved in methanol to make the same concentration. For the control experiment, methanol was added with DPPH. Finally, the absorbance values were measured and the antioxidant activities were calculated using the following equation (Thangavelu et al., 2018).

$$\% \text{ of antioxidant activity} = \frac{\text{Control OD} - \text{Experimental OD}}{\text{Control OD}} * 100$$

Where Control OD = Absorbance of the sample without Ag NPs; Experimental OD = Absorbance of the sample with Ag NPs. Results obtained were expressed as a percentage decrease with respect to DPPH control results. The results were plotted in the graph as a percentage of radical scavenging vs. concentrations of Ag NPs. The procedure was the same for the three ratios (1:1, 1:3, and 3:1) of Ag NPs.

4. RESULTS AND DISCUSSION

4.1. Phytochemical Analysis of the Leaf Extract

The Phytochemical test analysis is necessary to check the presence of compounds, such as phenols, alkaloids, terpenoids, flavonoids, glycosides, tannins, saponins, etc. The preparation of the *Foeniculum vulgare* leaf extract by aqueous extraction of the dried and ground plant was the initial activity carried out for the biosynthesis of the silver nanoparticle. Therefore; *Foeniculum vulgare* leaf extract is composed of phytochemicals that are capable of reducing the silver ions to silver nanoparticles by capping and stabilizing the formed nanoparticles. The results of the qualitative phytochemical analysis of the *Foeniculum vulgare* leaf extract are shown below in Table 3 and Figure 10. The data obtained revealed that the *Foeniculum vulgare* leaf is primarily composed of alkaloids, flavonoids, tannins, terpenoids, steroids, glycosides, benedicts, phenol, and saponins which are responsible for the facilitation of the biosynthesis of silver nanoparticles.

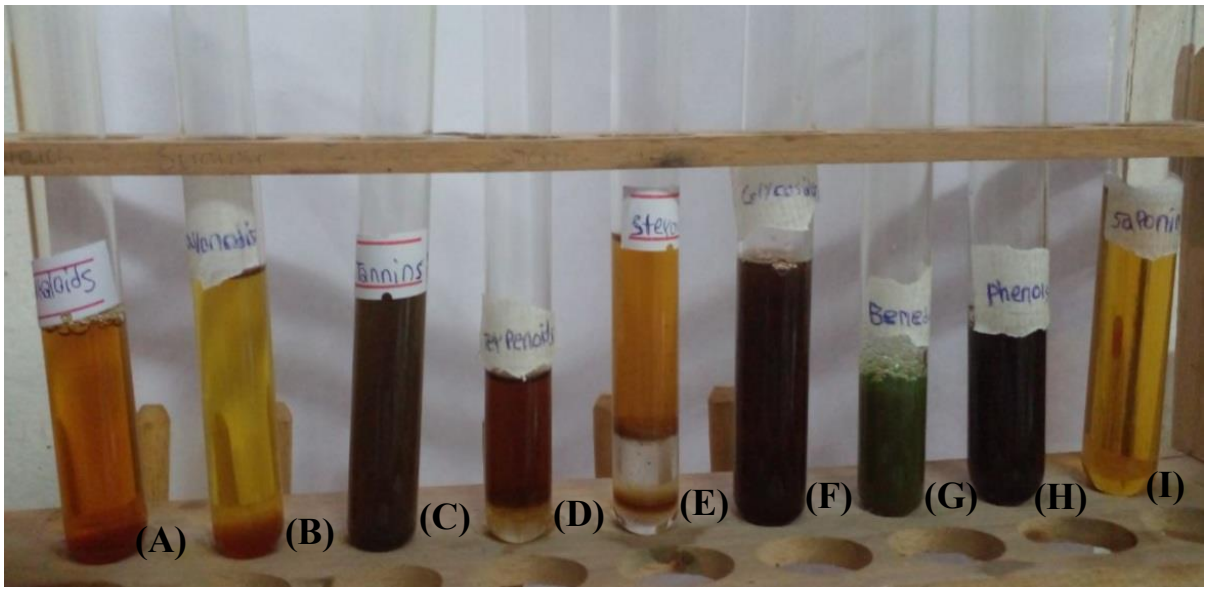

Figure 9. Phytochemical test colors are observed when the extract is tested for A). Alkaloid, B). Flavonoid, C). Tannins, D). Terpenoid, E). Steroid, F). Glycosides, G). Benedicts, H). Phenol, I). Saponins

Table 2. The qualitative analysis of Phytochemicals in the *Foeniculum vulgare* leaf extract.

No.	Phytoconstituents	Chemical test/reagent	Results	Colors observed
1	Alkaloid	Wagner's test	+	brown/reddish precipitate
2	Flavonoids	Alkaline Reagent Test	+	Yellow
3	Tannins	Ferric Chloride test	+	Brownish-green
4	Terpenoid	Salkowski test	+	reddish-brown
5	Steroid	Salkowski test	+	Red
6	Glycosides	Salkowski test	+	reddish-brown
7	Benedict	Benedict test	+	Blue-green
8	Phenols	Ferric Chloride test	+	Black
9	Saponins	Frothing test	+	Stable persistent froth

4.2. XRD Analysis of Biosynthesized Silver Nanoparticles

The X-ray diffraction (XRD) analysis was used to evaluate comprehensively the phase purity, average crystal size and details of the crystal structure of the produced silver nanoparticles. The analysis of the crystal phases and the average crystalline size of the synthesized silver nanoparticles prepared through the green method using *Foeniculum vulgare* leaf extract was done with an X-ray diffractometer.

The XRD diffraction spectrum of biosynthesized silver nanoparticles in 1:1, 1:3, and 3:1 ratios, respectively, shown in Figure 10, which demonstrates a total of four major peaks, ranging from 10° to 80° which displayed the peaks at 2θ values of 38.21°, 44.38°, 64.77°, and 77.58° and corresponds to hkl plane in a crystal lattice i.e., (111), (200), (220), and (311) crystallographic planes, respectively. The XRD analysis confirms that the prepared biosynthesized silver nanoparticles showed lattice planes of face-centered cubic crystalline structure with no impurities within the XRD instrument's detection limits.

Four maximum peaks at 2θ of 38.21°, 44.38°, 64.77°, and 77.58° with the intense peaks, and all the observed diffraction peaks show the formation of silver structure and matched with the literature value JCPD file no. 00-004-7383 (Fm3m), which confirms the purity of the

biosynthesized silver nanoparticles without the formation of any secondary phases and the result found to be in good agreement with the previously reported work (Ananda Murthy et al., 2020). For the three nanoparticles, all the observed peaks can be taken as confirmation of the formation of silver nanoparticles. This confirms that the intended biosynthesis of silver nanoparticles has been successful. Furthermore, the XRD pattern of biosynthesized silver nanoparticles shows sharp and intense peaks, indicating that the prepared samples were finely ground, homogenized with high crystalline quality, and average bulk composition is determined. The average crystallite sizes and lattice strain values for silver nanoparticles in the form of powder are determined by using Debye Scherrer's formula, which can be given in equation (1).

According to Scherrer's equation, the calculated average crystallite size of biosynthesized silver nanoparticles was found to be 21.61, 13.72, and 12.59 nm for the volume ratio of 1:1, 1:3, and 3:1, respectively, and the result is presented in Table 4. The characteristic peaks are higher in intensity which indicates that the products are good crystalline nature. As shown in Table 4 the average crystal sizes of the biosynthesized silver nanoparticles are all in the nano-range

According to (Zhang et al., 2016) the difference in particle sizes shown in Table 4 can be attributed to the silver nitrate salt concentration-dependent competition for nucleation and growth processes, as well as the electrostatic repulsion effect during the particle formation reaction. Among the three-volume ratio of silver nanoparticles 3:1 ratio has a small average crystallite size of 12.58 nm which is a smaller amount when compared to the average crystallite size of 1:1 and 1:3 ratio. This is because the greater amount of plant extract used during the synthesis process results in more capping, reducing/stabilizing agents, which effectively stabilize the biosynthesized silver nanoparticles during the synthesis process. The average crystalline size of the 3:1 ratio has less than that of the 1:3 ratio. This is because 3:1 has higher *Foeniculum vulgare* leaf extract and less precursor salt than that of 1:3. In 3:1 ratio lower concentrations of silver ions, the electrostatic repulsion factor is relatively less dominant, and the particle growth in such cases is primarily limited by the diffusion of species from solution to the growing surface of a particle.

In a 1:3 ratio, a high concentration of silver ions in the initial solution can produce smaller particle sizes due to higher electrostatic repulsion for the species migrating towards a growing particle. This ratio shows narrow diffraction peaks, indicating that it has a good crystalline structure as compared to the remaining two ratios; because it has small amounts of *Foeniculum vulgare* leaf extract and a high amount of precursor salt that is used during the synthesis process as a capping agent which fits with the porosity of the silver precursor salt and prevents aggregation of salts. The diffraction patterns of silver nanoparticles formed within a 1:1 volume ratio have sharp peak and high height, which shows that the material has a large average crystalline size when compared to the remaining two ratios and this ratio shows narrower than 1:3 and wider than 3:1; because it has an equal amount of leaf extract and precursor salt. Therefore X-ray diffraction of the silver nanoparticles revealed that the nanoparticles were crystalline and also confirms that they were capped by biomolecular compounds which were responsible for the reduction of silver ions.

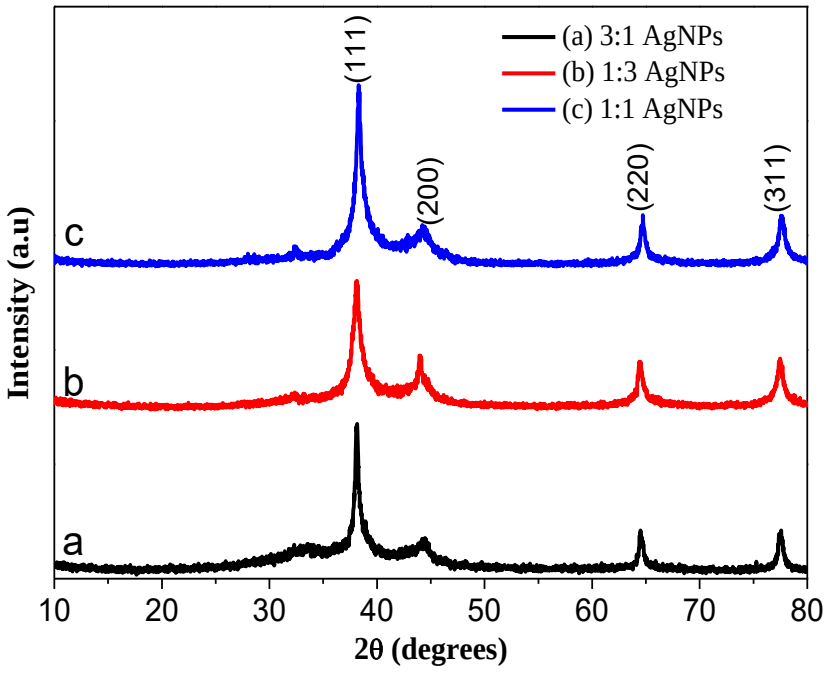

Figure 10. X-ray diffraction patterns silver nanoparticles biosynthesized under different volume ratios of Foeniculum vulgare leaf extract and silver nitrate salt (a) 3:1, (b) 1:3, (c) 1:1.

Table 3. Interplanar spaces (d-hkl), FWHM values, lattice parameter, and crystallite sizes of biosynthesized AgNPs.

Ag NPs 1:1							
2theta (2θ)	**Theta(θ)**	**FWMH (β)**	**hkl value**	**d_{hkl}**	**$(h^2+\kappa^2+l^2)^{1/2}$**	**Lattice parameter**	**crystallite sizes in nm**
38.1325	0.945141495	0.4453	111	4.669876505	1.73	8.088463371	19.714730
44.5110	0.925504152	0.44	200	4.768953031	2	9.537906063	20.375549
64.5204	0.845632812	0.425	220	5.219350607	2.83	14.76255283	23.087112
77.4742	0.780025388	0.4566	311	5.658316124	3.32	18.76651153	23.296771
Average Value (nm)						10.23108676	21.618541
Ag NPs 1:3							
2theta (2θ)	**Theta(θ)**	**FWMH (β)**	**hkl value**	**d_{hkl}**	**$(h^2+\kappa^2+l^2)^{1/2}$**	**Lattice parameter**	**crystallite sizes in nm**
38.3226	0.944598285	0.675	111	4.672561767	1.73	8.0931143	13.013360
44.2911	0.926229241	1.4266	200	4.765220032	2	9.5304400	6.2794220
64.6744	0.84491472	0.5633	220	5.223786206	2.83	14.775098	17.433627
77.5858	0.779415607	0.5867	311	5.662742678	3.32	18.781192	18.144925
Average Value (nm)						10.235969	13.717833
Ag NPs 3:1							
2theta (2θ)	**Theta(θ)**	**FWMH (β)**	**hkl value**	**d_{hkl}**	**$(h^2+\kappa^2+l^2)^{1/2}$**	**Lattice parameter**	**crystallite sizes in nm**
38.1218	0.945171993	0.8933	111	4.669725835	1.73	8.0882024	9.827254
44.0196	0.927119767	0.7967	200	4.760643293	2	9.5212865	11.23336
64.4429	0.845993612	0.68	220	5.217124816	2.83	14.756257	14.42329
77.4167	0.780339279	0.715	311	5.656040211	3.32	18.758963	14.87136
Average Value (nm)						10.2249419	12.58881

4.3. UV- Vis spectroscopy analysis of Biosynthesized Silver Nanoparticles

The optical properties of the biosynthesized silver nanoparticles are presented by characterizing via UV-Vis spectroscopy. As shown in Figure 11, the three-volume ratios of silver nanoparticles showed absorption peaks, recorded at the maximum wavelength of 336

nm, 334 nm, and 330 nm for 1:1, 1:3, and 3:1 of the biosynthesized silver nanoparticles respectively. Almost identical results were observed during the analysis of synthesized silver nanoparticles using the *Allium cepa* leaf extract (Abdellatif et al., 2022). The corresponding optical bandgap energy was calculated using Tauc's plot method which is discussed in equation (6) and was found to be 3.23, 3.35, and 3.51 eV for average nanoparticles of 21.6 nm, 13.7 nm, and 12.5 nm for 1:1, 1:3, and 3:1 volume ratios of leaf extract and silver precursor salt respectively, which indicated the presence of spherical silver nanoparticles. These results show that the energy band gap of silver nanoparticles may depend on its particle size (Table 5). The variation in the energy band gap for the different kinds of biosynthesized silver nanoparticles is due to the variation in volume ratio between silver precursor salt and the leaf extract that leads the biosynthesize silver nanoparticles to absorb at different regions of UV-Vis light. The band gap energy analysis confirmed the formation of silver nanoparticles which is in close agreement with previously reported values (Aziz et al., 2018). From the bandgap energy graph; as the bandgap energy decreases, average crystalline size increases, and the properties of nanoparticles are enhanced. The difference in the intensity and the band position of leaf extract and the biosynthesized silver nanoparticles is due to leaf extract yield (Jemal et al., 2017).

Table 4. Calculated bandgap for Ag NPs biosynthesized within 1: 1, 1: 3, and 3: 1 ratios.

Silver nanoparticles ratio	λmax (nm)	Bandgap (eV)	Average crystallite size
1:1	336	3.51	21.6
1:3	334	3.35	13.7
3:1	330	3.23	12.5

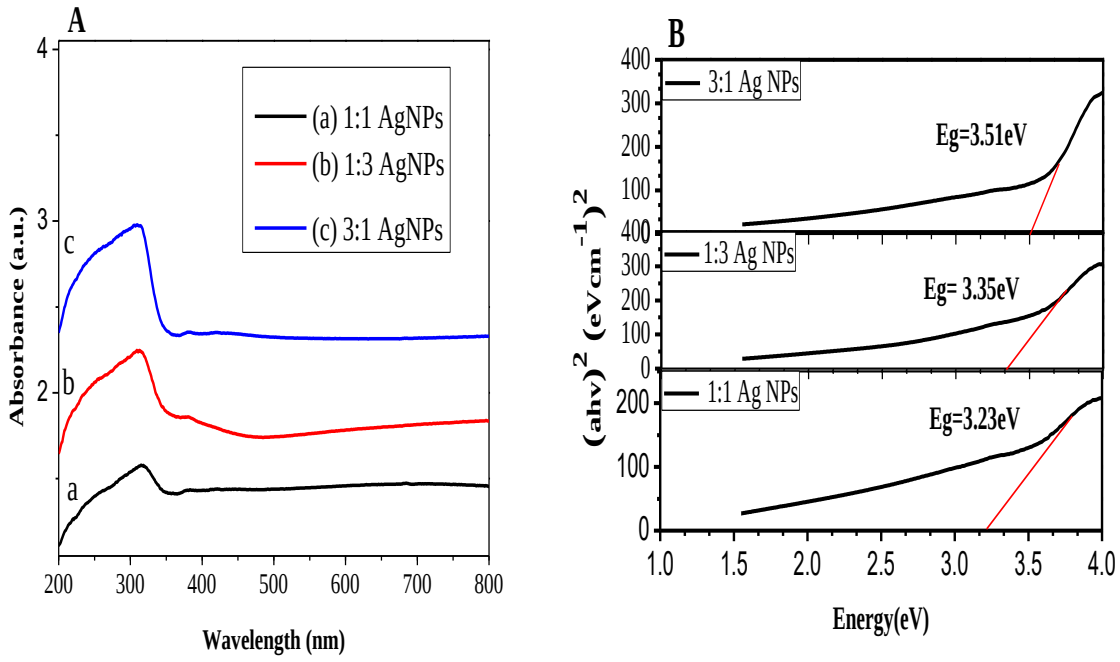

Figure 11. (A) Wavelength versus Absorbance of UV-Vis spectroscopy of Ag NPs, (B) Energy bandgap of the biosynthesized Ag NPs at different ratio.

4.4. FT-IR Analysis of Biosynthesized Silver Nanoparticles

FTIR analyses were performed to identify the potential functional groups of the biomolecules in the *Foeniculum vulgare* leaf extract and silver nanoparticles that are involved in capping, reduction of the silver ions to synthesize silver nanoparticles, and proficient stabilization of the synthesized silver nanoparticles. The FTIR spectroscopy helped reveal the bonding features of both the *Foeniculum vulgare* leaf extract and silver nanoparticles. Figure 12 shows the FTIR spectra of biosynthesized silver nanoparticles at a 1:1 volume ratio and the extracts of *Foeniculum vulgare* leaf powder were recorded in the range of 4000-500 cm^{-1}.

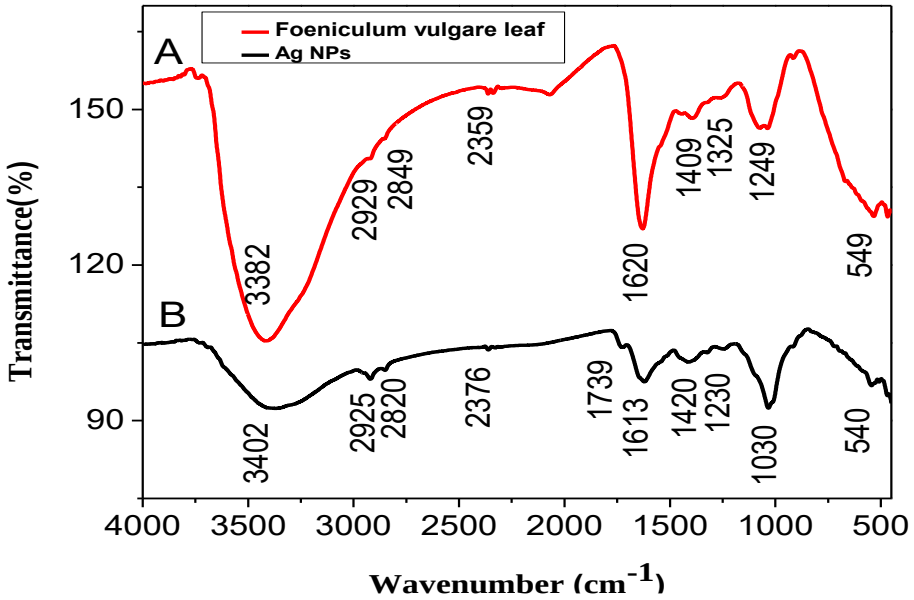

Figure 12. FT-IR spectra of biosynthesized Ag NPs and Foeniculum vulgare leaf extract.

The FTIR spectrum of *Foeniculum vulgare* leaf extract powder and biosynthesized silver nanoparticles were indicated in Figures 12 (a) and (b), respectively. Absorption bands at 3382, 2929, 2849, 2359, 1620, 1409, 1325, 1249, and 549 cm^{-1}. The FTIR spectra of obtained nanoparticles show different absorption bands ranging from 3382 to 549 cm^{-1}, which indicate the presence of some active functional groups. The broad absorption intense peaks are shown in Fig 12, respectively at 3382 cm^{-1} and 1249 cm^{-1} corresponding to phenolic–OH stretching. This very broad O-H stretch band is observed with a C=O peak, which almost certainly indicates that the compound is an aliphatic carboxylic acid (Salmen & Alharbi, 2020).

The small intense peaks shown at 2929 cm^{-1} and 2849 cm^{-1} correspond to asymmetric –C–H stretching of $–CH_2$ and $–CH_3$ groups and –C–N group of secondary amines. These two functional groups showed the presence of the saponin functional group (Widyaningtyas et al., 2019). The vibration of–COO group of carboxylic acid was found to appear at 1409 cm^{-1} (Azarbani & Shiravand, 2020). The C-C bond stretching at the aromatic ring was found to appear at 1325. The presence of –COOH stretching vibration was located at a wave number of 2359 cm^{-1}. It also reveals carbonyl group bonds present in the leaf extract of *Foeniculum vulgare*, indicating protein binding with the surface of silver and thus leading to the stabilization of the biosynthesized nanoparticles (that is capping of Ag NPs) and used to

prevent agglomeration. The absorption peaks represented at 1620 cm^{-1} indicates the presence of C=O vibration of ketonic groups and C=C bending mode of vibrations, which indicate the presence of flavonoid compounds (Jemal et al., 2017). A peak at 549 cm^{-1} correlates to bending vibrations of the C–H bond (Siva Kumar et al., 2013).

In Figure 12 (b), the absorption peaks were observed at 3402 cm^{-1}, 2925 cm^{-1}, 2820 cm^{-1}, 2376 cm^{-1}, 1739 cm^{-1}, 1613 cm^{-1}, 1420 cm^{-1}, 1230 cm^{-1}, 1030 cm^{-1} and 540 cm^{-1} with some small shifts for the biosynthesized silver nanoparticles. The broad absorption band observed at 3402 cm^{-1} represents O-H bond stretching, which is phenol is due to adsorbed moisture at the surface of silver nanoparticles which is phenol, and the weak absorption band at 2376cm^{-1} is due to C=O bond stretching that could be emanated from the presence of adsorbed carbon dioxide on the surface of nanoparticles. The peaks at 2925 cm^{-1} and 2820 cm^{-1} were due to the presence of C–H symmetrical stretching of hydrocarbons such as alkanes and aldehydes (Gude et al., 2013). The band at 1613 cm^{-1} corresponds to N-H bending indicating the presence of secondary amines (Prakash et al., 2013). The band at 1420 cm^{-1} was due to the presence of CH_2 and CH_3 bend stretch which showed the presence of the alkanes. As reported in many studies these functional groups have a role in the capping/stability of silver nanoparticles (Prakash et al., 2013).

The bands at 1030 cm^{-1} correspond to the C– O stretch vibration of the alkyl ketone compound, respectively. According to (Balaji et al., 2009; Mandal et al., 2005), the carbonyl groups of the amino acid residues and the peptides, free amino, or cysteine groups in proteins can bind to the silver. The band at 1230 cm^{-1} was assigned to the C – O stretching of alkyl ketone. The FTIR spectrum of silver nanoparticles absorbs at 540 cm^{-1}. The peak in (Table 7) showed the functional group determined by FT-IR. The FTIR spectra of both leaf extract and silver nanoparticles indicate the presence of bioactive molecules around the silver nanoparticles such as alkaloids, phenols, flavonoids, amino acids, glycosides, and tannins are responsible for the biotransformation of silver ions to silver nanoparticles and its stabilization in an aqueous medium. These bioactive molecules had been confirmed to have performed a sizable function in the nucleation and growth of silver nanoparticles.

Table 5.The FTIR spectrum of *Foeniculum vulgare* leaf extract powder.

Wavenumber (cm^{-1})	Functional group	Compound class	Intensity
3382	O-H stretching	Alcohols	Broad, strong
2929	Aldehyde CH stretching	Alkanes	Medium
2849	C - H stretching	Aldehydes	Strong
2359	-COOH stretching	Carboxyl	Strong
1620	C = C bending/C=O vibration	flavonoid/ ketonic compounds	Strong
1409	Vibration of –COO	carboxylic acid	Strong
1325	C-C stretching	Aromatic ring	Weak
1249	C-O stretching	Alkyl ketone	Strong
549	C-X	Halo alkane	Weak

Table 6.The characteristic of FT-IR for the biosynthesized Ag NPs.

Wavenumber (cm^{-1})	Functional group	Compound class	Intensity
3402	O-H stretching	Alcohols	Broad, strong
2925	Aldehyde CH stretching	Alkanes	Medium
2820	C - H stretching	Aldehydes	strong
2376	C = O stretching	Carbonyl group	Strong
1739	C = O stretching	Carbonyl group	Strong
1613	N – H bend	Secondary amines	Weak to medium
1420	CH_2 and CH_3 bend	Alkanes	Weak
1230	C-O stretching	Alkyl ketone	Strong
1030	C – O stretching	Alkyl ketone	Strong
540	C-X	Halo alkane	Weak

Therefore, as a result of the FTIR analyses of the biosynthesized Ag NPs, can be concluded that some of the biological molecules of leaf extracts confirmed the presence of phytochemicals (alkaloid, phenolics, flavonoids, tannins, terpenoids, glycosides, and so on) in leaf extract and their roles as reducing and stabilizing agents during Ag NPs synthesis.

Especially the phenolics were reported to be strong candidates for binding with Ag NPs (Ananda Murthy et al., 2020).

4.5. SEM Analysis of Biosynthesized Silver Nanoparticles

The surface morphology (texture) and the size distribution of the biosynthesized Ag NPs were determined using SEM images. The SEM results confirmed the microstructural features, morphologies, and shape of Ag NPs were dependent on the mixing ratio of leaf extract of *Foeniculum vulgare* and silver nitrate under the same reaction conditions. Figure 13 shows Ag NPs with different volume ratios of 1:1, 1:3, and 3:1, respectively. As observed in Figure 13 (A, B) 1:1 ratio of Ag NPs are less agglomerated due to the presence of an equal amount of *Foeniculum vulgare* leaf extract precursor salt solution. In Figure 13 (C, D) 1:3 ratio of Ag NPs confirm a good combination of biomolecules obtained from the leaf extract with Ag NPs during the synthesis process, and the presence of the leaf extract coats the surface of the Ag NPs thus preventing from aggregation (Of et al., 2019). The efficient role of biomolecules as stabilizing agents prevents the growth of clusters of silver atoms into bigger NPs. In Figure 13 (E, F) 3:1 ratio of Ag NPs show agglomeration which results due to the presence of the excess amount of leaf extract of *Foeniculum vulgare*, which was beyond the coating surface of silver nanoparticles (Mudalige et al., 2020).

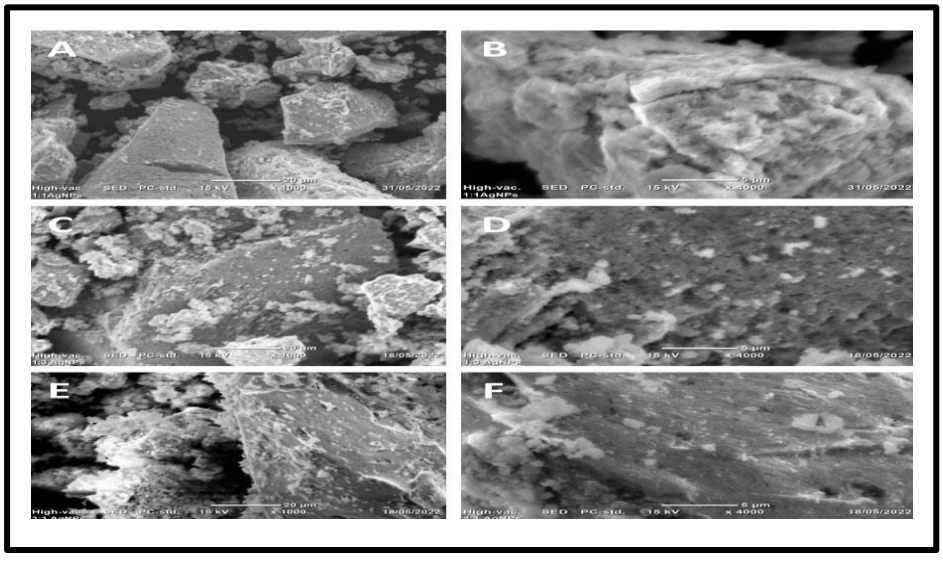

Figure 13.The SEM image of silver nanoparticles (A and B) 1:1, (C and D) 1:3, and (E and F) 3:1 ratios, with two different magnifications (5 and 20 μm).

4.6. Antibacterial Activity Analysis of Biosynthesized Silver Nanoparticles

The antibacterial activity of the biosynthesized Ag NPs in three volume ratios was investigated against both the two gram-positive (*Staphylococcus aureus* ATCC25923 and *Streptococcus Pyogenes* ATCC19615) and two gram-negative bacteria *(Pseudomonas aeuruginosa* ATCC27853 and *Escherichia coli* ATCC25923*)* through the disc diffusion method. Amoxicillin was used as a positive control. The zone of inhibition values indicated that all the Ag NPs exhibited a varied range of 7.5-13.5 mm of antibacterial activities against all the tested bacterial strains. In comparison, the antibacterial activity of Ag NPs at 50 μg/mL, and 75 μg/mL, was weaker than at 100 μg/mL suggesting that the activity displayed has a dose-dependent manner (Table 8). Table 8, Figures 14, and 16 show the antibacterial activity of Ag NPs biosynthesized within three different volumes such as 1:1, 1:3, and 3:1 ratios.

From the three ratios of biosynthesized silver nanoparticles, 3:1 showed better performance on the antibacterial activity as compared to 1:1 and 1:3 ratios. In a 3:1 ratio, the range of zone of inhibition was between 9-13.5 mm (Table 8). This could be due to the smaller average crystalline size and the presence of higher concentrations of bioactive compounds found in the leaf extract. It indicates that the high antibacterial performance contributed due to the high ROS production. Then the high ROS production results from the use of the large volume of *Foeniculum vulgare* extract which contains amounts of OH radical.

1:1 ratio showed the second most strong activity with a maximum zone of inhibition of 11, 12.5, 11.5, and 11 mm at the concentration of 100 μg/mL.10, 10, 10, and, 10.5 mm at the concentration of 75 μg/mL. 9, 8.5, 9, and 19 mm at the concentration of 50 μg/mL against *S. aureus, P. aeruginosa, E. coli,* and *S. pyogenes,* respectively. 1:1 silver nanoparticles showed good performance followed by a 3:1 volume ratio that exists the bioactive compound within an equal ratio of metal salt and interacts with the surface of the bacteria cell wall and to penetrate it. In a 1:1 volume ratio, the range of zone of inhibition was between 8.5-12.5 mm. A maximum zone of inhibition of 12.5 mm was produced against *Streptococcus pyogen,* at the concentration of 100 μg/mL. The least zone of inhibition was observed in *Pseudomonas aeruginosa* at 50 μg/mL (Figure 14. and Table 8.). This might be due to the larger average crystalline nature of the formed silver nanoparticles in its XRD spectrum as compared to the

other ratios. In this ratio, the bioactive compound is found within an equal ratio of precursor salt and then interacts with the surface of the bacteria cell wall and penetrates to it. 1:3 ratio showed weak activity comparably, with a zone of inhibition of 11, 11, 10.5, and 10 mm at the concentration of 100 μg/mL. 9.5, 10, 9, and 19 mm at the concentration of 75 μg/mL. 9, 8, 8, and 7.5 mm at the concentration of 50 μg/mL against *S. aureus, P. aeruginosa, E. coli,* and *S. pyogenes,* respectively.

In the 1:3 volume ratio, the range of zone of inhibition was between 7.5-11 mm. A maximum zone of inhibition of 11 mm was produced against *Streptococcus pyogen* and, *Staphylococcus aureus* at the concentration of 100 μg/mL. The least zone of inhibition was observed in *Pseudomonas aeruginosa* at 50 μg/mL (Figure 14. and Table 8.). 1:3 volume ratio showed the least performance on the antibacterial activity as compared to 1:1 and 3:1volume ratios because of their large surface area, which allows for better contact with the cell wall of bacteria, silver nanoparticles demonstrated antibacterial activity. Depending on our result, the antibacterial activity of biosynthesized silver nanoparticles in three volume ratio was found to increase with an increase in the amount of *Foeniculum vulgare* leaf extracts as shown in Figure 16 and Table 8. When the concentration of silver nanoparticles is 50 μg/mL, 75 μg/mL, and 100 μg/mL increase the zone of inhibition also increases within the three-volume ratios. The order of inhibition was as follows: 3:1 ratio>1:1 ratio>1:3 ratio.

The result indicated that *Staphylococcus aureus* and *Streptococcus pyogen* (Gram-positive) bacteria have high antibacterial activity when compared to *Pseudomonas aeuruginosa* and *Escherichia coli* (Gram-negative) bacteria in the three ratios (Figure 15). This might be due to *Staphylococcus aureus* and *Streptococcus pyogen* bacteria having a thick peptidoglycan layer whereas *Pseudomonas aeuruginosa* and *Escherichia coli* bacteria have thinner peptidoglycan but are surrounded by a lipid layer outside. The literature report revealed silver nanoparticles can easily attach to the bacterial cell wall and then penetrate the bacteria and disturb the permeability of the cell membrane and causing intracellular Adenosine triphosphate (ATP) leakage and the bacterial cell's death. A previous study obtained similar results (Azarbani & Shiravand, 2020; Pirtarighat et al., 2019).

Table 7. Antibacterial activity of Ag NPs biosynthesized within 1: 1, 1: 3, and 3: 1 ratios.

Compound and Conc.n (mg/mL) of Ag NPs		Bacterial strains and Zone of Inhibition in mm			
		S.aureus ATCC25923	*S. Pyogenes* ATCC19615	*E. coli* ATCC25923	*P. aeruginosa* ATCC27853
1:3	A1=50 µg/mL	9	8	8	7.5
	A2=75 µg/mL	9.5	10	9	9
	A3=100 µg/mL	11	11	10.5	10
3:1	B1=50 µg/mL	10.5	11	10	9
	B2=75 µg/mL	12	12.5	12	12
	B3=100 µg/mL	13.5	13.5	12.5	12
1:1	C1=50 µg/mL	9	8.5	9	9
	C2=75 µg/mL	10	10	10	10.5
	C3=100 µg/mL	11	12.5	11.5	11
	Amoxicillin	14	14	12.5	13

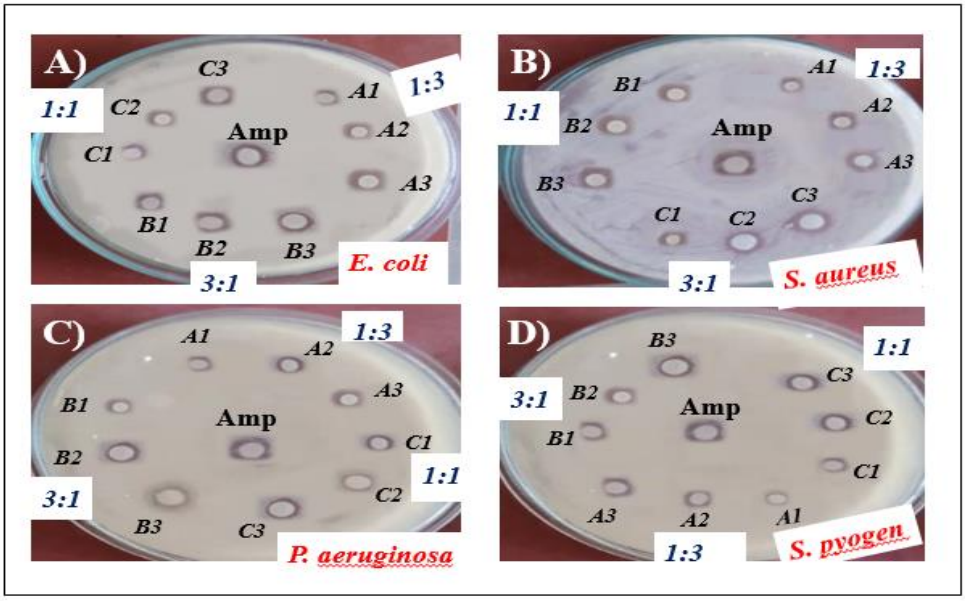

Figure 14. Disc diffusion antibacterial activity evaluation of the biosynthesized silver nanoparticles 1:1, 1:3, and 3:1 ratio against *P. aeruginosa*, *S. pyogenes*, *E. coli*, and *S. aureus*.

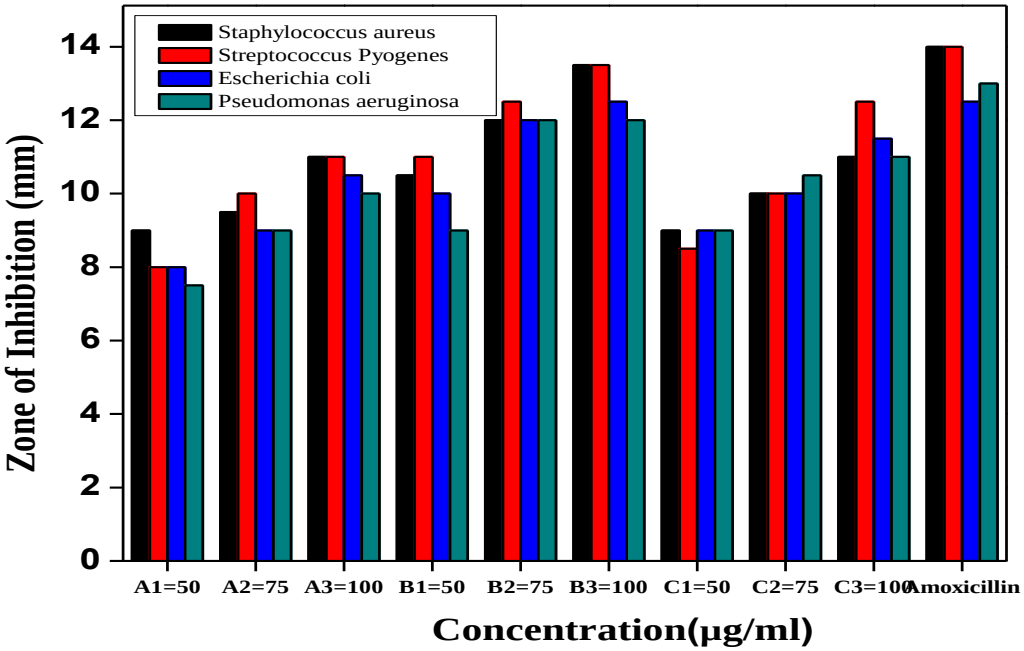

Figure 15. The zone of inhibition of Ag NPs and Amoxicillin (+ve cont) against bacterial strains gram-negative, *E.coli and P. aeruginosa* and gram-positive, *S. pyogenes and S.aureus.*

4.7. Antifungal Activity Analysis of Biosynthesized Silver Nanoparticles

The antifungal activity of the biosynthesized Ag NPs was tested against two fungal strains *Aspergillus niger* (AN) and *Candidca albicans* (CA). The zone of inhibition (ZOI) was measured at different concentrations of 15 mg/mL, 20 mg/mL, and 25 mg/mL in three ratios. The result is shown in Figure 16 and Table 9. Antifungal activity was shown by an inhibition zone which was characterized by a clear zone between the wells (containing samples) and a certain distance. The zone of inhibition values indicated that all the compounds and concentrations of silver nanoparticles exhibited a varied range of 0-16 mm of antifungal activities against all the tested fungal strains. The formation of inhibition zones around the wells shows fungal sensitivity to antifungal and antibiotic ingredients (which are used as positive controls). The positive control used in the well was a ketoconazole/Tilt (10 units/disc) and functioned as a control of the test solution by comparing the diameter of the inhibition zone formed. In comparison, the antifungal activity of compounds and concentration of silver nanoparticles at 15, and 20 mg/mL was weaker than at 25 mg/mL suggesting that the activity displayed has a dose-dependent manner (Table 9). As Table 9 shows when the concentration of Ag NPs 15 mg/mL, 20 mg/mL, and 25 mg/mL increases zone of inhibition was increased respectively.

Aspergillus niger showed strong activity in a 3:1 ratio with a maximum zone of inhibition of 12.5 ± 3.46, 14.3 ± 4.70, and 16.9 mm at the concentrations of 15, 20, and 25 mg/mL, respectively. The second strongest activity showed at a 1:3 ratio with a maximum zone of inhibition of 7, 8.5 ± 0.5, and 11.2 ± 0.28 mm at the concentration of 15, 20, and 25 mg/mL, respectively. 1:1 ratio showed weak activity comparably, with a zone of inhibition 2 ± 0.5, 5.5 ± 0.40, and 10 ± 0.11 mm at the concentration 0f 15, 20 and 25 mg/mL, respectively. At 15 and 20 mg/mL, it does not show antifungal activity. *Candida albicans* showed strong activity in a 3:1 ratio with a maximum zone of inhibition of 10.1 ± 0.59, 14.2 ± 0.25, and 16.1 ± 0.5 mm at the concentrations of 15, 20, and 25 mg/mL, respectively. The second strongest activity showed at a 1:3 ratio with a maximum zone of inhibition of 6.6 ± 0.85, 7.4 ± 0.76, and 10.5 ± 0.26 mm at the concentrations of 15, 20, and 25 mg/mL, respectively. 1:1 ratio showed weak activity comparably, with a zone of inhibition of 0, 5, and 8.3 ± 0.26 mm at the concentration of 15, 20, and 25 mg/mL, respectively.

Among the different ratios of the biosynthesized Ag NPs, Ag (3: 1) nanoparticles showed better performance of antifungal activity as compared to the remaining two ratios (1:3 and 1:1). This might be due to the smaller average crystalline size and also the difference in the volume of capping agents obtained from the leaf extract of *Foeniculum vulgare*. Biosynthesized Ag NPs within a volume ratio of 1: 3 show more resistance towards *Aspergillus niger* than *Candida albicans*. This might be because of the morphology of the biosynthesized Ag NPs shows agglomeration which results in lowering the in vitro antifungal activity. The antifungal activity against *Aspergillus niger* was increased, which was indicated by an increase in the inhibition zone diameter from 2 mm to 16.9 mm, with an increasing Ag NPs of 25 mg/mL. The fungal species *Candida albicans* had shown medium sensitivity to silver nanoparticles with a concentration of 25 mg/mL, whereas the *Aspergillus niger* fungal species showed good sensitivity to the Ag NPs concentration of 25 mg/mL (Table 9). This may be due to the individual organism's response and their genotypic characteristics which differs in their sensitivity pattern towards the single testing agent. The result showed that the Ag NPs can disrupt the cell membrane structure and then penetrate into the fungi which leads to cell death (Farrag et al., 2020).

Table 8. Antifungal activity of Ag NPs biosynthesized within 1: 1, 1: 3, and 3: 1 ratios.

concentration of Ag NPs (mg/mL)		Fungal strains and zone of inhibition in mm ± SD			
		Aspergillus niger		*Candida albicans*	
		Mean ± SD	Ketoconazole	Mean ± SD	Ketoconazole
3:1	15 mg/Ml	12.5 ± 3.46	22	10.1± 0.59	21
	20 mg/Ml	14.3 ± 4.70		14. 2 ± 0.25	
	25 mg/mL	16.9		16. 1 ± 0.5	
1:3	15 mg/Ml	7	20	0	15
	20 mg/Ml	8.5 ± 0.5		5	
	25 mg/Ml	11.2 ± 0.28		8. 3 ± 0.25	
1:1	15 mg/mL	2 ± 0.5	18	6.6 ± 0.85	16
	20 mg/mL	5.5 ± 0.40		7.4 ± 0.76	
	25 mg/mL	10± 0.11		10.5 ± 0.26	

1, 2 and 3 represents 15 mg/mL, 20 mg/mL, and 25 mg/mL respectively.

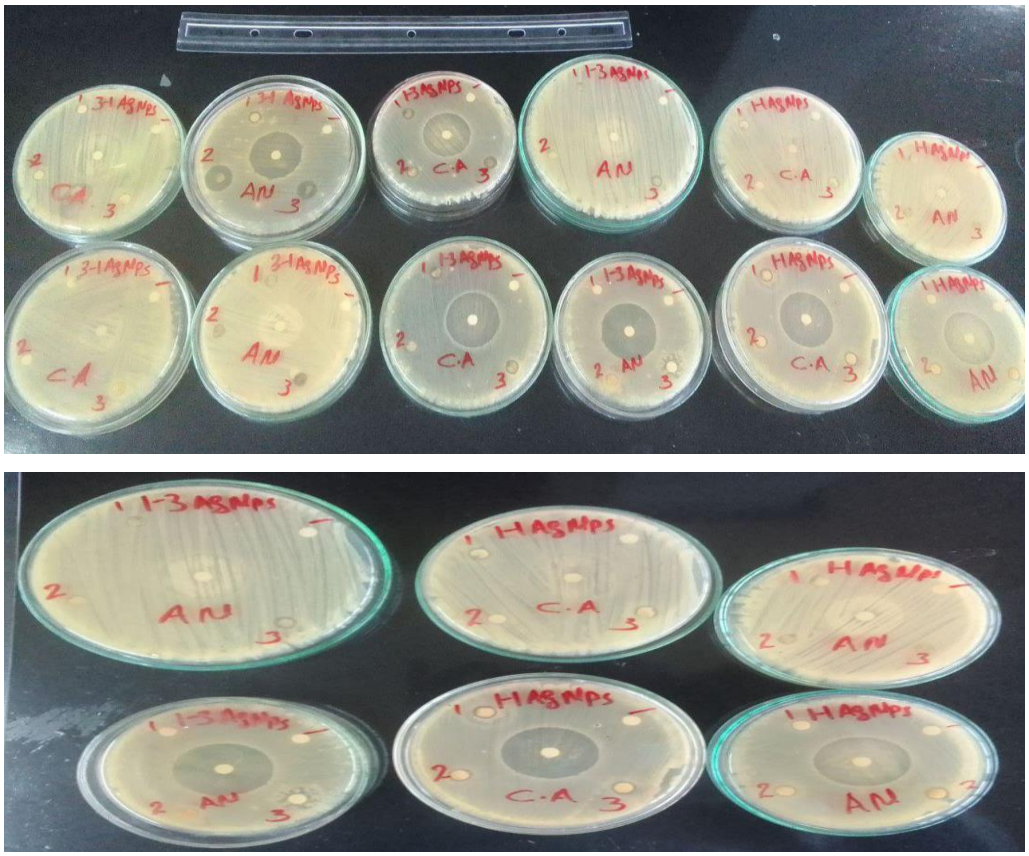

Figure 16. Disc diffusion antifungal activity evaluation of the biosynthesized silver nanoparticles 1:1, 1:3, and 3:1 ratio against *Aspergillus niger* (AN) and *Candida albicans* (CA).

4.8. Antioxidant Activity Analysis of Biosynthesized Silver Nanoparticles

The DPPH assay was used to assess the free radical scavenging activity of the biosynthesized silver nanoparticles. DPPH antioxidant assay is based on the ability of 2, 2-diphenyl-1-picryl-hydrazyl (DPPH), a stable free radical, to decolorize in the presence of antioxidants. The DPPH radical contains an odd electron, which is responsible for the absorbance at 517 nm and also for a visible deep purple color. A decrease in the absorbance of the reaction mixture indicates significant free radical scavenging activity of the compound under test. In vitro, an antioxidant assay of silver nanoparticles revealed the presence of antioxidant potential. The percentage of inhibition was observed in all the antioxidant models that free radicals were scavenged by the

synthesized silver nanoparticles in a concentration-dependent manner up to the given concentration. The data are compared to those obtained with the reference ascorbic acid. The relationship between different analogues of the biosynthesized silver nanoparticles and their scavenging activity for the DPPH radical is shown in table 10. All of the investigated substances showed moderate to high radical scavenging activities compared with the absorbance of the control (1.099). The DPPH radical-scavenging activities at 800 µg/mL were 42.4%, 27.3% and 28.9% for 1:1, 1:3, and 3:1 silver nanoparticles ratios, respectively. The order of inhibition was as follows: 1:1 ratio > 3:1 ratio > 1:3ratio. The 1:1 ratio of silver nanoparticles showed a significantly higher percentage of inhibition and the 3:1 ratio of silver nanoparticles scored the second most potent percentage of inhibition whilst the 1:3 ratio of silver nanoparticles displayed a lower percentage of inhibition of DPPH. Therefore, as the concentration increases the percentage of antioxidant potential also increases. The antioxidant potential was compared with the standard antioxidant (ascorbic acid).

The significant antioxidant potential of silver nanoparticles was evaluated by DPPH radical scavenging assay. Among the different concentrations (50, 100, 200, 400, and 800 µg/mL) of *Foeniculum vulgare* nanoparticles were tested for antioxidant activity, and the leaf synthesized nanoparticles showed activity from 50–800 µg/L in the DPPH assay. These silver nanoparticles are capable to scavenge the purple color 2, 2-diphenyl-1- picrylhydrazyl (DPPH) radicals. The antioxidant activity shows in the concentration dependant manner to inhibit the free radicals. Interestingly, the higher concentration of silver nanoparticles produced a high percentage of antioxidant potential than the lower concentration. This is shown in the three ratios.

From the three different volume ratios 3:1 silver nanoparticles ratios showed better antioxidant activity when compared to 1:1 and 1:3 silver nanoparticles ratios this is due to the presence of plant leaf extract. As Figure 17 shows when the concentration of the three different volume ratios of silver nanoparticles and the positive control Ascorbic acid increases from 50 to 800 µg/mL the absorbance was decreases. The biosynthesized silver nanoparticles showed a good ability as radical scavengers in investigations using the DPPH method. In comparison to Keshari *et al*., report, the antioxidant activity reported here is good (Keshari et al., 2020).

Table 9. Antioxidant activity of Ag NPs biosynthesized within 1: 1, 1: 3, and 3: 1 ratio and Ascorbic acid.

Conc. (µg/mL)	Control	Ratios						Positive control	
		1:1 Ag NPs		1:3 Ag NPs		3:1 Ag NPs		Ascorbic Acid	
	Abs	Abs	%RSA	Abs	%RSA	Abs	%RSA	Abs	%RSA
800	1.099	0.633	42.40218	0.798	27.38854	0.781	28.9354	0.024	97.8162
400	1.099	0.774	29.57234	0.808	26.47862	0.795	27.66151	0.037	96.6333
200	1.099	0.86	21.74704	0.832	24.29481	0.837	23.83985	0.073	93.3576
100	1.099	0.903	17.83439	0.853	22.38399	0.851	22.56597	0.121	88.98999
50	1.099	0.916	16.6515	0.889	19.10828	0.855	22.202	0.135	87.71611

Abs= Absorbance; Conc. = Concentration; %RSA= Radical scavenging activity.

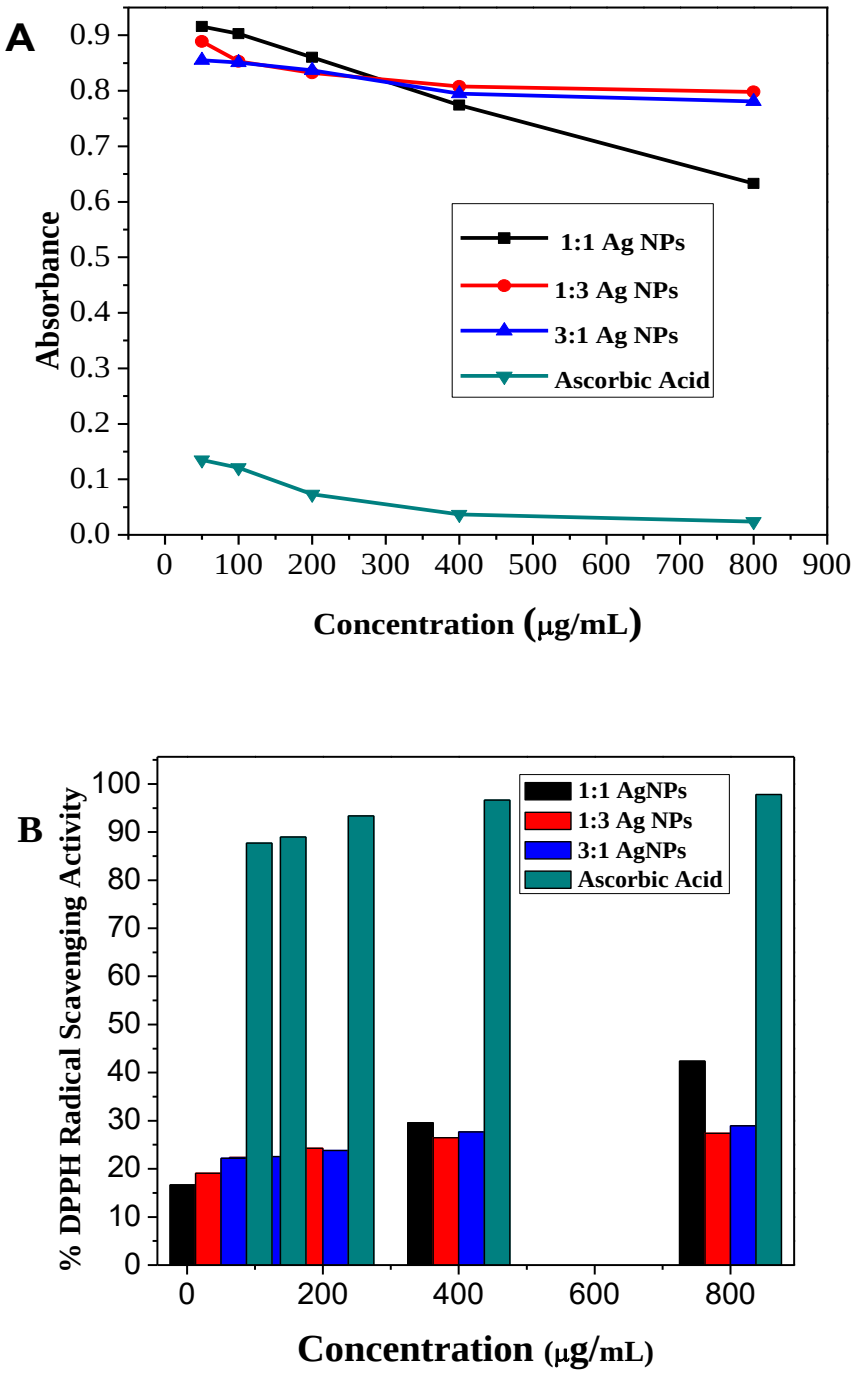

Figure 17. (A) The DPPH assay of concentration versus absorbance, (B) Antioxidant potential of Ag NPs biosynthesized within 1: 1, 1: 3, and 3: 1 ratio and Ascorbic acid.

5. CONCLUSIONS AND RECOMMENDATIONS

5.1. Conclusions

In this work, silver nanoparticles were successfully biosynthesized using silver nitrate as a precursor in the presence of *Foeniculum vulgare* leaf extract within different ratios 1:1, 1:3, and 3:1. The biosynthesized silver nanoparticles were then characterized by XRD, UV-Vis, SEM, and FT-IR Spectroscopy. More crystalline nature and best performing silver nanoparticles were obtained when it was biosynthesized within a 3: 1 ratio. Crystalline analysis showed the average crystalline size as 21.61, 13.72, and 12.59 nm for 1:1, 1:3, and 3:1, respectively. The XRD result confirmed the face-centered cubic crystal structure of silver nanoparticles. The maximum absorption wavelengths were recorded at 336, 334, and 330 nm for 1:1, 1:3, and 3:1 silver nanoparticles respectively. The energy bandgap values for 1:1, 1:3, and 3:1 silver nanoparticles were found to be 3.23, 3.35, and 3.51 eV, respectively. The nearly spherical morphology of the biosynthesized silver nanoparticles was confirmed by SEM micrographs. The surface bonding features were confirmed by FT-IR analysis. Functional group analysis indicates the presence of various capping and stabilizing agents. The in vitro antibacterial activity of the biosynthesized three ratios of silver nanoparticles and leaf extract of *Foeniculum vulgare* was investigated. Among the different ratios of silver nanoparticles, (the 3:1 ratio) has better performing the antimicrobial activity. This is due to its small average crystalline size, uniform spherical shape, and large surface region, which creates electronic effects, and these effects can increase the binding strength of the nanoparticles with the bacteria cell membrane. The antibacterial studies of biosynthesized silver nanoparticles conducted against the gram-negative species, *E. coli*, and *P. aeruginosa*, and gram-positive species, *S. pyogenes*, and *S. aureus* revealed more efficiency for silver nanoparticles. The antifungal studies of biosynthesized silver nanoparticles conducted against *Candida albicans and Aspergillus niger* revealed more efficiency for silver nanoparticles. Among the different ratios of silver nanoparticles, (the 1:1 ratio) has better performing the antioxidant activity. The antioxidant activities displayed by the silver nanoparticles were significant compared with ascorbic acid demonstrating the potential antioxidant activity.

5.2. Recommendations

This research study used the green method for the synthesis of silver nanoparticles which is eco-friendly nature and environmentally harmless. Silver nanoparticle synthesis through green methods is one of the emerging research areas with huge future prospective. Since the silver nanoparticles displayed potent antimicrobial and antioxidant activity, it is necessary to evaluate other activities including anticancer, optoelectronic devices, electrochemical activity, Photocatalytic activity, biomedical applications, and other activities. Green synthesized silver nanoparticles could be tested for the removal of toxic and heavy metal ions from industries and real waste/sludge/. The antimicrobial activity of green synthesized silver nanoparticles could be enhanced it will be done in the presence of UV light. To apply practically, researchers may include health center staff such as doctors, pharmacists, and so on.

REFERENCE

Abdel-aziz, M. S., Shaheen, M. S., & El-nekeety, A. A. (2013). Antioxidant and antibacterial activity of silver nanoparticles biosynthesized using Chenopodium murale leaf extract. *JOURNAL OF SAUDI CHEMICAL SOCIETY*. https://doi.org/10.1016/j.jscs.2013.09.011

Abdel-haleem, F. M., Mahmoud, S., Abdel-ghani, N. E. T., Mohamed, R., Nashar, E., Bechelany, M., & Barhoum, A. (2021). *Polyvinyl Chloride Modified Carbon Paste Electrodes for Sensitive Determination of Levofloxacin Drug in Serum , Urine , and Pharmaceutical Formulations*.

Abdellatif, A. A. H., Mahmood, A., Alsharidah, M., Mohammed, H. A., Alenize, S. K., Bouazzaoui, A., Al Rugaie, O., Alnuqaydan, A. M., Ahmad, R., Vaali-Mohammad, M. A., Alfayez, M., Traiki, T. Bin, Al-Regaiey, K. A., Ali, A. T., Hassan, Y. A. H., & Abdulla, M. H. (2022). Bioactivities of the Green Synthesized Silver Nanoparticles Reduced Using Allium cepa L Aqueous Extracts Induced Apoptosis in Colorectal Cancer Cell Lines. *Journal of Nanomaterials*, *2022*. https://doi.org/10.1155/2022/1746817

Abdulsahib, S. S. (2021). Synthesis, characterization and biomedical applications of silver nanoparticles. *Biomedicine (India)*, *41*, 458–464. https://doi.org/10.51248/.v41i2.1058

Aisida, S. O., Ugwu, K., Akpa, P. A., Nwanya, A. C., Nwankwo, U., Botha, S. S., Ejikeme, P. M., Ahmad, I., Maaza, M., & Ezema, F. I. (2019). Biosynthesis of silver nanoparticles using bitter leave (Veronica amygdalina) for antibacterial activities. *Surfaces and Interfaces*, *17*(July), 100359. https://doi.org/10.1016/j.surfin.2019.100359

Al-Hadid, K. J. (2017). Quantitative analysis of antimicrobial activity of Foeniculum vulgare. A review. *Plant OMICS*, *10*(1), 28–36. https://doi.org/10.21475/poj.10.01.17.322

Alabi, J., & Huisman, R. K. (2012). *Collaborative Librarianship By and for Us : The Development of a Program for Peer Review of Teaching by and for Pre-Tenure Librarians By and for Us : The Development of a Program for Peer Review of Teaching by*. *4*(4).

Ali, M. E., Das, R., Eaqub, A., Bee, S., & Hamid, A. (2014). Current Applications of X-Ray Powder. *Rev. Adv. Mater. Sci*, *38*, 95–109. www.scopus.com

Ali, Z. A., Yahya, R., Sekaran, S. D., & Puteh, R. (2016). *Green Synthesis of Silver Nanoparticles Using Apple Extract and Its Antibacterial Properties*. *2016*.

Allah, A., & Mohanta, T. K. (2020). *Nanoparticles Synthesized by The Reducing Activity of Plants i v o r l a n o i v o l*. https://doi.org/10.3389/fmicb.2020.01143

Ananda Murthy, H. C., Desalegn Zeleke, T., Ravikumar, C. R., Anil Kumar, M. R., & Nagaswarupa, H. P. (2020). Electrochemical properties of biogenic silver nanoparticles synthesized using Hagenia abyssinica (Brace) JF. Gmel. medicinal plant leaf extract. *Materials Research Express*, *7*(5). https://doi.org/10.1088/2053-1591/ab9252

Anbu, P., Gopinath, S. C. B., Yun, H. S., & Lee, C. G. (2019). Temperature-dependent green biosynthesis and characterization of silver nanoparticles using balloon flower plants and their antibacterial potential. *Journal of Molecular Structure*, *1177*, 302–309. https://doi.org/10.1016/j.molstruc.2018.09.075

Azarbani, F., & Shiravand, S. (2020). Green synthesis of silver nanoparticles by Ferulago macrocarpa flowers extract and their antibacterial, antifungal and toxic effects. *Green Chemistry Letters and Reviews*, *13*(1), 41–49. https://doi.org/10.1080/17518253.2020.1726504

Aziz, A., Khalid, M., Akhtar, M. S., Nadeem, M., Gilani, Z. A., Ul Huda Khan Asghar, H. M. N., Rehman, J., Ullah, Z., & Saleem, M. (2018). Structural, Morphological and Optical Investigations of Silver Nanoparticles Synthesized By Sol-Gel Auto-Combustion Method. *Digest Journal of Nanomaterials and Biostructures*, *13*(3), 679–683.

Babatunde, D. E., Denwigwe, I. H., Babatunde, O. M., & Saheed, L. (2019). Environmental and Societal Impact of Nanotechnology. *IEEE Access*, *PP*, 1. https://doi.org/10.1109/ACCESS.2019.2961513

Badgujar, S. B., Patel, V. V., & Bandivdekar, A. H. (2014). Foeniculum vulgare Mill: A review of its botany, phytochemistry, pharmacology, contemporary application, and toxicology. *BioMed Research International*, *2014*. https://doi.org/10.1155/2014/842674

Balaji, D. S., Basavaraja, S., Deshpande, R., & Mahesh, D. B. (2009). *Colloids and Surfaces B : Biointerfaces Extracellular biosynthesis of functionalized silver nanoparticles by strains of Cladosporium cladosporioides fungus*. *68*, 88–92.

https://doi.org/10.1016/j.colsurfb.2008.09.022

Bano, I., & Deora, G. S. (2019). Preliminary phytochemical screening and GC-MS analysis of methanolic leaf extract of Abutilon pannosum (Forst. F.) Schlect. from Indian Thar desert. *Journal of Pharmacognosy and Phytochemistry*, *8*(1), 894–899.

Barhoum, A., Pal, K., Rahier, H., Uludag, H., & Kim, I. S. (n.d.). *Nanofibers as New-Generation Materials : From Spinning and Nano-Spinning Fabrication Techniques to Emerging Applications*.

Basavaraja, S., Balaji, S. D., Lagashetty, A., Rajasab, A. H., & Venkataraman, A. (2008). Extracellular biosynthesis of silver nanoparticles using the fungus Fusarium semitectum. *Materials Research Bulletin*, *43*(5), 1164–1170. https://doi.org/10.1016/j.materresbull.2007.06.020

Batsatsashvili, K., Kikvidze, Z., & Bussmann, R. (2020). *Ethnobotany of the Mountain Regions of Far Eastern Europe: Ural, Northern Caucasus, Turkey, and Iran.*

Begum, R., Farooqi, Z. H., Naseem, K., Ali, F., Batool, M., Xiao, J., & Irfan, A. (2018). Applications of UV/Vis Spectroscopy in Characterization and Catalytic Activity of Noble Metal Nanoparticles Fabricated in Responsive Polymer Microgels: A Review. *Critical Reviews in Analytical Chemistry*, *48*(6), 503–516. https://doi.org/10.1080/10408347.2018.1451299

Bengal, W. (2013). *Anatomical variation in the olfactory apparatus of marine teleosts*. *3*(1).

Beyazen, A., Dessalegn, E., & Mamo, W. (2017). Phytochemical Screening and Biological Activities of Leaf of Foeniculum vulgare (Ensilal). *World Journal of Agricultural Sciences*, *13*(1), 1–10. https://doi.org/10.5829/idosi.wjas.2017.01.10

Boobalan, T., Raja, R., Anand, K., & Sudhakar, M. (2018). US. *Journal of Photochemistry & Photobiology, B: Biology*, #pagerange#. https://doi.org/10.1016/j.jphotobiol.2018.07.021

Cabral, C., Miranda, M., Gonçalves, M. J., Cavaleiro, C., Cruz, M. T., & Salgueiro, L. (2017). Assessment of safe bioactive doses of Foeniculum vulgare Mill. essential oil from Portugal. *Natural Product Research*, *31*(22), 2654–2659. https://doi.org/10.1080/14786419.2017.1292266

Chou, K. Sen, Lu, Y. C., & Lee, H. H. (2005). Effect of alkaline ion on the mechanism and

kinetics of chemical reduction of silver. *Materials Chemistry and Physics*, *94*(2–3), 429–433. https://doi.org/10.1016/j.matchemphys.2005.05.029

Chouhan, N. (2018). Silver Nanoparticles: Synthesis, Characterization and Applications. *Silver Nanoparticles - Fabrication, Characterization and Applications*. https://doi.org/10.5772/intechopen.75611

Consumption, G., Challenges, F., Salim, M. R., Kueh, A. H., Hadibarata, T., & Nur, H. (2017). *A Review of Silver Nanoparticles: Research Trends, Global Consumption, Synthesis, Properties, and Future Challenges Achmad Sya fi uddin,*. 732–756. https://doi.org/10.1002/jccs.201700067

Cp, K. (2017). Phytochemical analysis and total phenol content in Daucus carota Linn. *International Journal of Advanced Science and Research*, *2*(6), 74–76.

Dakal, T. C., Kumar, A., Majumdar, R. S., & Yadav, V. (2016). Mechanistic basis of antimicrobial actions of silver nanoparticles. *Frontiers in Microbiology*, *7*(NOV), 1–17. https://doi.org/10.3389/fmicb.2016.01831

Das, C. G. A., Kumar, V. G., Dhas, T. S., Karthick, V., Govindaraju, K., Joselin, J. M., & Baalamurugan, J. (2020). Biocatalysis and Agricultural Biotechnology Antibacterial activity of silver nanoparticles (biosynthesis): A short review on recent advances. *Biocatalysis and Agricultural Biotechnology*, *27*, 101593. https://doi.org/10.1016/j.bcab.2020.101593

de Aragão, A. P., de Oliveira, T. M., Quelemes, P. V., Perfeito, M. L. G., Araújo, M. C., Santiago, J. de A. S., Cardoso, V. S., Quaresma, P., de Souza de Almeida Leite, J. R., & da Silva, D. A. (2019). Green synthesis of silver nanoparticles using the seaweed Gracilaria birdiae and their antibacterial activity. *Arabian Journal of Chemistry*, *12*(8), 4182–4188. https://doi.org/10.1016/j.arabjc.2016.04.014

Desalegn, T., Ravikumar, C. R., & Murthy, H. C. A. (2020). *Eco-friendly synthesis of silver nanostructures using medicinal plant Vernonia amygdalina Del. leaf extract for multifunctional applications*. *January 2021*. https://doi.org/10.1007/s13204-020-01620-7

Dessie, Y., Tadesse, S., & Eswaramoorthy, R. (2020). Physicochemical parameter influences and their optimization on the biosynthesis of MnO2 nanoparticles using Vernonia

amygdalina leaf extract. *Arabian Journal of Chemistry*, *13*(8), 6472–6492. https://doi.org/10.1016/j.arabjc.2020.06.006

Dhand, V., Soumya, L., Bharadwaj, S., Chakra, S., Bhatt, D., & Sreedhar, B. (2016). Green synthesis of silver nanoparticles using Coffea arabica seed extract and its antibacterial activity. *Materials Science and Engineering C*, *58*, 36–43. https://doi.org/10.1016/j.msec.2015.08.018

Din, M. I., Arshad, F., Hussain, Z., & Mukhtar, M. (2017). *Green Adeptness in the Synthesis and Stabilization of Copper Nanoparticles : Catalytic , Antibacterial , Cytotoxicity , and Antioxidant Activities*. https://doi.org/10.1186/s11671-017-2399-8

Durán, N., Durán, M., de Jesus, M. B., Seabra, A. B., Fávaro, W. J., & Nakazato, G. (2016). Silver nanoparticles: A new view on mechanistic aspects on antimicrobial activity. *Nanomedicine: Nanotechnology, Biology, and Medicine*, *12*(3), 789–799. https://doi.org/10.1016/j.nano.2015.11.016

Ealias, A. M., & Saravanakumar, M. P. (2017). A review on the classification, characterisation, synthesis of nanoparticles and their application. *IOP Conference Series: Materials Science and Engineering*, *263*(3). https://doi.org/10.1088/1757-899X/263/3/032019

Egbuna, C., Ifemeje, J. C., Udedi, S. C., & Kumar, S. (2019). Phytochemistry, Volume 1: Fundamentals, Modern Techniques, and Applications. In *Journal of Chemical Information and Modeling* (Vol. 1).

Endalamaw, F. D., & Chandravanshi, B. S. (2015). Levels of major and trace elements in fennel (Foeniculum vulgari Mill.) fruits cultivated in Ethiopia. *SpringerPlus*, *4*(1), 1–10. https://doi.org/10.1186/2193-1801-4-5

Esmaile, F., Koohestani, H., & Abdollah-Pour, H. (2020). Characterization and antibacterial activity of silver nanoparticles green synthesized using Ziziphora clinopodioides extract. *Environmental Nanotechnology, Monitoring and Management*, *14*(April), 100303. https://doi.org/10.1016/j.enmm.2020.100303

Esquivel-Ferriño, P. C., Favela-Hernández, J. M. J., Garza-González, E., Waksman, N., Ríos, M. Y., & Del Rayo Camacho-Corona, M. (2012). Antimycobacterial activity of constituents from Foeniculum vulgare var. Dulce Grown in Mexico. *Molecules*, *17*(7),

8471–8482. https://doi.org/10.3390/molecules17078471

Farrag, H. M. M., Mostafa, F. A. A. M., Mohamed, M. E., & Huseein, E. A. M. (2020). Green biosynthesis of silver nanoparticles by Aspergillus niger and its antiamoebic effect against Allovahlkampfia spelaea trophozoite and cyst. *Experimental Parasitology*, *219*, 108031. https://doi.org/10.1016/j.exppara.2020.108031

Felici, E., & Raba, J. (2015). Author ' s Accepted Manuscript. *Talanta*. https://doi.org/10.1016/j.talanta.2015.08.060

Fissan, H., Ristig, S., Kaminski, H., Asbach, C., & Epple, M. (2014). Comparison of different characterization methods for nanoparticle dispersions before and after aerosolization. *Analytical Methods*, *6*(18), 7324–7334. https://doi.org/10.1039/c4ay01203h

Foti, M. C. (2015). Use and Abuse of the DPPH• Radical. *Journal of Agricultural and Food Chemistry*, *63*(40), 8765–8776. https://doi.org/10.1021/acs.jafc.5b03839

Ganbarov, K. G., Agayeva, N. A., Ramazanov, M. A., & Abdulhamidova, S. M. (2016). Extracellular Formation of Silver Nanoparticles by the Cell Filtrate of Actinomyces spp. NSX-333. *International Journal of Research Studies in Biosciences*, *4*(11), 57–60. https://doi.org/10.20431/2349-0365.0411009

Ganesh, K. N., Zhang, D., Miller, S. J., Rossen, K., Chirik, P. J., Kozlowski, M. C., Zimmerman, J. B., Brooks, B. W., Savage, P. E., Allen, D. T., & Voutchkova-Kostal, A. M. (2021). Green Chemistry: A Framework for a Sustainable Future. *ACS Sustainable Chemistry and Engineering*. https://doi.org/10.1021/acssuschemeng.1c03891

Garg, P., Garg, R., & Praveen Garg, C. (2019). Phytochemical screening and quantitative estimation of total flavonoids of Ocimum sanctum in different solvent extract. *~ 16 ~ The Pharma Innovation Journal*, *8*(2), 16–21. www.thepharmajournal.com

Ghotekar, S., Pansambal, S., Pawar, S. P., Pagar, T., Oza, R., & Bangale, S. (2019). Biological activities of biogenically synthesized fluorescent silver nanoparticles using Acanthospermum hispidum leaves extract. *SN Applied Sciences*, *1*(11). https://doi.org/10.1007/s42452-019-1389-0

Gude, V., Upadhyaya, K., Prasad, M. N. V, & Rao, N. V. S. (2013). *Green Synthesis of Gold and Silver Nanoparticles Using*. *5*(3), 223–228.

https://www.hindawi.com/journals/jnt/2013/906592/

Gudimalla, A., Jose, J., Rajendran, J. V., Gurram, G., & Thomas, S. (2021). Synthesis of silver nanoparticles by plant extract, incorporated into alginate films and their characterizations. *Chemical Papers*, *0123456789*. https://doi.org/10.1007/s11696-021-01923-1

Gudimalla, A., Jose, J., Varghese, R. J., & Thomas, S. (2021). Green Synthesis of Silver Nanoparticles Using Nymphae odorata Extract Incorporated Films and Antimicrobial Activity. *Journal of Polymers and the Environment*, *29*(5), 1412–1423. https://doi.org/10.1007/s10924-020-01959-6

Guilger-casagrande, M., & Lima, R. De. (2019). *Synthesis of Silver Nanoparticles Mediated by Fungi : A Review*. *7*(October), 1–16. https://doi.org/10.3389/fbioe.2019.00287

Harish, V., Tewari, D., Gaur, M., Yadav, A. B., & Swaroop, S. (2022). *Review on Nanoparticles and Nanostructured Materials : Bioimaging , Biosensing , Drug Delivery , Tissue Engineering , Antimicrobial , and Agro-Food Applications*.

Hasnain, M. S., Javed, N., Alam, S., & Rishishwar, P. (2019). Materials Science & Engineering C Purple heart plant leaves extract-mediated silver nanoparticle synthesis : Optimization by Box-Behnken design. *Materials Science & Engineering C*, *99*(January), 1105–1114. https://doi.org/10.1016/j.msec.2019.02.061

Huston, M., Debella, M., Dibella, M., & Gupta, A. (2021). Green synthesis of nanomaterials. *Nanomaterials*, *11*(8), 12–14. https://doi.org/10.3390/nano11082130

Ibrahim, E., Fouad, H., Zhang, M., & Zhang, Y. (2019). *endophytic bacteria and their role in inhibition of promotion*. 29293–29299. https://doi.org/10.1039/c9ra04246f

Irshad, A., Sarwar, N., Sadia, H., Riaz, M., Sharif, S., Shahid, M., & Khan, J. A. (2020). Silver nano-particles: synthesis and characterization by using glucans extracted from Pleurotus ostreatus. *Applied Nanoscience (Switzerland)*, *10*(8), 3205–3214. https://doi.org/10.1007/s13204-019-01103-4

Jadhav, K., Deore, S. L., Dhamecha, D., Hr, R., Jagwani, S., Jalalpure, S. S., & Bohara, R. A. (2018). *Phytosynthesis of silver nanoparticles : characterization , biocompatibility studies and anticancer activity*. https://doi.org/10.1021/acsbiomaterials.7b00707

Jemal, K., Sandeep, B. V., & Pola, S. (2017). Synthesis, Characterization, and Evaluation of

the Antibacterial Activity of Allophylus serratus Leaf and Leaf Derived Callus Extracts Mediated Silver Nanoparticles. *Journal of Nanomaterials*, *2017*. https://doi.org/10.1155/2017/4213275

Jiang, L., Santiago, I., Foord, J. S., & Accepted, J. (2020). *High-Yield Electrochemical Synthesis of Silver Nanoparticles at Enzyme-Modified Boron-Doped Diamond Electrode*. https://doi.org/10.1021/acs.langmuir.0c00375

Jubu, P. R., Yam, F. K., Igba, V. M., & Beh, K. P. (2020). Tauc-plot scale and extrapolation effect on bandgap estimation from UV–vis–NIR data – A case study of β-Ga2O3. *Journal of Solid State Chemistry*, *290*(July), 121576. https://doi.org/10.1016/j.jssc.2020.121576

Jung, J. H., Cheol Oh, H., Soo Noh, H., Ji, J. H., & Soo Kim, S. (2006). Metal nanoparticle generation using a small ceramic heater with a local heating area. *Journal of Aerosol Science*, *37*(12), 1662–1670. https://doi.org/10.1016/j.jaerosci.2006.09.002

Keshari, A. K., Srivastava, R., Singh, P., Yadav, V. B., & Nath, G. (2020). Antioxidant and antibacterial activity of silver nanoparticles synthesized by Cestrum nocturnum. *Journal of Ayurveda and Integrative Medicine*, *11*(1), 37–44. https://doi.org/10.1016/j.jaim.2017.11.003

Kgatshe, M., Aremu, O. S., Katata-seru, L., & Gopane, R. (2019). *Characterization and Antibacterial Activity of Biosynthesized Silver Nanoparticles Using the Ethanolic Extract of Pelargonium sidoides DC*. *2019*.

Khan, M. Z. H., Tareq, F. K., Hossen, M. A., & Roki, M. N. A. M. (2018). *GREEN SYNTHESIS AND CHARACTERIZATION OF SILVER NANOPARTICLES USING CORIANDRUM SATIVUM LEAF EXTRACT*. *13*(1), 158–166.

Khodadadi, S., Mahdinezhad, N., Fazeli-Nasab, B., Heidari, M. J., Fakheri, B., & Miri, A. (2021). Investigating the Possibility of Green Synthesis of Silver Nanoparticles Using Vaccinium arctostaphlyos Extract and Evaluating Its Antibacterial Properties. *BioMed Research International*, *2021*. https://doi.org/10.1155/2021/5572252

Kim, M., Osone, S., Kim, T., Higashi, H., & Seto, T. (2017). Synthesis of nanoparticles by laser ablation: A review. *KONA Powder and Particle Journal*, *2017*(34), 80–90. https://doi.org/10.14356/kona.2017009

Kiss, F. D., Miotto, R., & Ferraz, A. C. (2011). *Size effects on silver nanoparticles ’*. *275708*. https://doi.org/10.1088/0957-4484/22/27/275708

Kumar, A., Srivastava, R., Singh, P., & Bahadur, V. (2020). Journal of Ayurveda and Integrative Medicine Antioxidant and antibacterial activity of silver nanoparticles synthesized by Cestrum nocturnum. *Journal of Ayurveda and Integrative Medicine*, *11*(1), 37–44. https://doi.org/10.1016/j.jaim.2017.11.003

Kumar, B., Smita, K., Cumbal, L., Debut, A., & Pathak, R. N. (2014). *Sonochemical Synthesis of Silver Nanoparticles Using Starch : A Comparison*. *2014*.

Lagashetty, A., Ganiger, S. K., Preeti, R. K., & Reddy, S. (2021). Green synthesis, characterization and antibacterial study of ag-au bimetallic nanocomposite using tea powder extract. *Biointerface Research in Applied Chemistry*, *11*(1), 8087–8095. https://doi.org/10.33263/BRIAC111.80878095

Lakshmi, Y. S., Banu, F., & Gopalakrishnan, S. (2013). *Green Synthesis , And Antimicrobial Activity Of Silver Nanoparticles From The Medicinal Plant Vernonia Amygdalina*. *2*, 3–6.

Li, P., Liu, N., Yu, H., Wang, F., Liu, L., Lee, G., & Wang, Y. (2016). Silver nanostructures synthesis via optically induced electrochemical deposition. *Nature Publishing Group*, *May*, 1–8. https://doi.org/10.1038/srep28035

Lin, P. C., Lin, S., Wang, P. C., & Sridhar, R. (2014). Techniques for physicochemical characterization of nanomaterials. *Biotechnology Advances*, *32*(4), 711–726. https://doi.org/10.1016/j.biotechadv.2013.11.006

MALLMANN, E. J. J., CUNHA, F. A., CASTRO, B. N. M. F., MACIEL, A. M., MENEZES, E. A., & FECHINE, P. B. A. (2015). Antifungal Activity of Silver Nanoparticles Obtained By Green Synthesis. *Revista Do Instituto de Medicina Tropical de São Paulo*, *57*(2), 165–167. https://doi.org/10.1590/s0036-46652015000200011

Mandal, S., Phadtare, S., & Sastry, M. (2005). *Interfacing biology with nanoparticles*. *5*(July 2004), 118–127. https://doi.org/10.1016/j.cap.2004.06.006

Manuscript, A. (2018). *Biomaterials Science*. https://doi.org/10.1039/C8BM00021B

Meena, P. R., Singh, A. P., & Tejavath, K. K. (2020). *Biosynthesis of Silver Nanoparticles*

Using Cucumis prophetarum Aqueous Leaf Extract and Their Antibacterial and Antiproliferative Activity Against Cancer Cell Lines. https://doi.org/10.1021/acsomega.0c00155

Mehra, N., Tamta, G., & Nand, V. (2021). A review on nutritional value, phytochemical and pharmacological attributes of Foeniculum vulgare Mill. *Journal of Pharmacognosy and Phytochemistry*, *10*(2), 1255–1263. https://doi.org/10.22271/phyto.2021.v10.i2q.13983

Mehra, N., Tamta, G., Nand, V., & Biswas, S. (2021). Compositional analysis of Foeniculum vulgare seeds genotypes collected from Tarai region of Uttarakhand. *The Pharma Innovation*, *10*(1), 268–271. https://doi.org/10.22271/tpi.2021.v10.i1d.5524

Mlalila, N. G., Swai, H. S., Hilonga, A., & Kadam, D. M. (2017). Antimicrobial dependence of silver nanoparticles on surface plasmon resonance bands against Escherichia coli. *Nanotechnology, Science and Applications*, *10*, 1–9. https://doi.org/10.2147/NSA.S123681

Modi, J. (2018). A Review on Synthesis of Silver NPS from Natural Source and their Applications. *Research & Development in Material Science*, *9*(1), 2014–2015. https://doi.org/10.31031/rdms.2018.09.000702

Mohammed, A. B. A., Mohamed, A., El-Naggar, N. E. A., Mahrous, H., Nasr, G. M., Abdella, A., Ahmed, R. H., Irmak, S., Elsayed, M. S. A., Selim, S., Elkelish, A., Alkhalifah, D. H. M., Hozzein, W. N., & Ali, A. S. (2022). Antioxidant and Antibacterial Activities of Silver Nanoparticles Biosynthesized by Moringa oleifera through Response Surface Methodology. *Journal of Nanomaterials*, *2022*(Ccd). https://doi.org/10.1155/2022/9984308

Mohammed, A. E. (2015). Green synthesis, antimicrobial and cytotoxic effects of silver nanoparticles mediated by Eucalyptus camaldulensis leaf extract. *Asian Pacific Journal of Tropical Biomedicine*, *5*(5), 382–386. https://doi.org/10.1016/S2221-1691(15)30373-7

Mohanta, Y. K., Panda, S. K., Jayabalan, R., & Sharma, N. (2017). *Antimicrobial , Antioxidant and Cytotoxic Activity of Silver Nanoparticles Synthesized by Leaf Extract of Erythrina suberosa (Roxb .)*. *4*(March), 1–9. https://doi.org/10.3389/fmolb.2017.00014

Mohd Radzuan, N. A., Sulong, A. B., & Sahari, J. (2017). A review of electrical conductivity models for conductive polymer composite. *International Journal of Hydrogen Energy*, *42*(14), 9262–9273. https://doi.org/10.1016/j.ijhydene.2016.03.045

Momin, B., Rahman, S., Jha, N., & Annapure, U. S. (2019). Valorization of mutant Bacillus licheniformis M09 supernatant for green synthesis of silver nanoparticles : photocatalytic dye degradation , antibacterial activity , and cytotoxicity. *Bioprocess and Biosystems Engineering*, *0*(0), 0. https://doi.org/10.1007/s00449-018-2057-2

Mudalige, K., Gayanthika, K., Kuruppu, P., Shashika, A., & Kuruppu, S. (2020). Characterization of spherical Ag nanoparticles synthesized from the agricultural wastes of Garcinia mangostana and Nephelium lappaceum and their applications as a photo catalyzer and fluorescence quencher. *SN Applied Sciences*, *2*(12), 1–24. https://doi.org/10.1007/s42452-020-03640-y

Nisha, N., & Suja, S. (2018). Phyto chemical evalution and antioxidant activity of methanol extract of Loligo duvauceli Ink. *Journal of Pharmacognosy and Phytochemistry*, *7*(1), 1764–1767.

Núñez, R. N., Veglia, A. V., & Lorena, N. (2018). Improving reproducibility between batches of silver nanoparticles using an experimental design approach. *Microchemical Journal*, #pagerange#. https://doi.org/10.1016/j.microc.2018.05.017

Nzekekwu, A. K., & Abosede, O. O. (2019). Green synthesis and characterization of silver nanoparticles using leaves extracts of neem (*Azadirachta indica*) and bitter leaf (*Vernonia amygdalina*). *Journal of Applied Sciences and Environmental Management*, *23*(4), 695. https://doi.org/10.4314/jasem.v23i4.19

Of, I., Plants, D., On, E., Nanoparticles, S., & Synthesis, G. (2019). *Three plants extracts were used for biosynthesis of Ag nanoparticles (AgNPs). AgNPs nucleation process requires effective reduction agents which secure Ag + to Ag 0 reduction and also stabilizing/capping agents. The UV-vis and TEM observation revealed tha*. *64*, 665–670. https://doi.org/10.24425/amm.2019.127596

Pal, G., Rai, P., & Pandey, A. (2019). Green synthesis of nanoparticles: A greener approach for a cleaner future. In *Green Synthesis, Characterization and Applications of Nanoparticles*. Elsevier Inc. https://doi.org/10.1016/b978-0-08-102579-6.00001-0

Pandey, S., Goswami, G. K., & Nanda, K. K. (2012). International Journal of Biological Macromolecules Green synthesis of biopolymer – silver nanoparticle nanocomposite : An optical sensor for ammonia detection. *International Journal of Biological Macromolecules*, *51*(4), 583–589. https://doi.org/10.1016/j.ijbiomac.2012.06.033

Paper, C., & Haider, A. (2018). *A review on preparation of silver nano-particles*. *June*. https://doi.org/10.1063/1.5039273

Patra, J. K., & Baek, K. H. (2014). Green Nanobiotechnology: Factors Affecting Synthesis and Characterization Techniques. *Journal of Nanomaterials*, *2014*. https://doi.org/10.1155/2014/417305

Paula, A., Melo, Z. De, Vinicius, M., Brisola, D. O., & Sganzerla, W. G. (2020). *Antibacterial activity , morphology , and physicochemical stability of biosynthesized silver nanoparticles using thyme (Thymus vulgaris) essential oil Antibacterial activity , morphology , and physicochemical stability of biosynthesized silver nanoparti*.

Pirtarighat, S., Ghannadnia, M., & Baghshahi, S. (2019). Green synthesis of silver nanoparticles using the plant extract of Salvia spinosa grown in vitro and their antibacterial activity assessment. *Journal of Nanostructure in Chemistry*, *9*(1), 1–9. https://doi.org/10.1007/s40097-018-0291-4

Prabhu, S., & Poulose, E. K. (2012). Silver nanoparticles: mechanism of antimicrobial action, synthesis, medical applications, and toxicity effects. *International Nano Letters*, *2*(1), 1. https://doi.org/10.1186/2228-5326-2-32

Prakash, P., Gnanaprakasam, P., Emmanuel, R., Arokiyaraj, S., & Saravanan, M. (2013). Green synthesis of silver nanoparticles from leaf extract of Mimusops elengi, Linn. for enhanced antibacterial activity against multi drug resistant clinical isolates. *Colloids and Surfaces B: Biointerfaces*, *108*, 255–259. https://doi.org/10.1016/j.colsurfb.2013.03.017

Preetha, D., Arun, R., Kumari, P., & Aarti, C. (2013). Synthesis and characterization of silver nanoparticles using cannonball leaves and their cytotoxic activity against Mcf-7 cell line. *Journal of Nanotechnology*, *2013*, 1–5.

Pryshchepa, O., Pomastowski, P., & Buszewski, B. (2020). Silver nanoparticles: Synthesis, investigation techniques, and properties. *Advances in Colloid and Interface Science*, *284*,

87–100. https://doi.org/10.1016/j.cis.2020.102246

Quinn, P. S., & Benzonelli, A. (2018). XRD and Materials Analysis. *The Encyclopedia of Archaeological Sciences*, 1–5. https://doi.org/10.1002/9781119188230.saseas0619

Quintero-quiroz, C., Acevedo, N., Zapata-giraldo, J., Botero, L. E., Quintero, J., Zárate-triviño, D., Saldarriaga, J., & Pérez, V. Z. (2019). *Optimization of silver nanoparticle synthesis by chemical reduction and evaluation of its antimicrobial and toxic activity*. 1–15.

Quinteros, M. A., Bonilla, J. O., Alborés, S. V., Villegas, L. B., & Páez, P. L. (2019). Biogenic nanoparticles: Synthesis, stability and biocompatibility mediated by proteins of Pseudomonas aeruginosa. *Colloids and Surfaces B: Biointerfaces*, *184*(May), 110517. https://doi.org/10.1016/j.colsurfb.2019.110517

Rafique, M., Sadaf, I., Rafique, M. S., & Tahir, M. B. (2017). A review on green synthesis of silver nanoparticles and their applications. *Artificial Cells, Nanomedicine and Biotechnology*, *45*(7), 1272–1291. https://doi.org/10.1080/21691401.2016.1241792

Rajeshkumar, S., & Bharath, L. V. (2017). Mechanism of plant-mediated synthesis of silver nanoparticles – A review on biomolecules involved, characterisation and antibacterial activity. *Chemico-Biological Interactions*, *273*, 219–227. https://doi.org/10.1016/j.cbi.2017.06.019

Rajoriya, P., Misra, P., Singh, V. K., Shukla, P. K., & Ramteke, P. W. (2017). Green Synthesis of Silver Nanoparticles. *Biotech Today : An International Journal of Biological Sciences*, *7*(1), 7. https://doi.org/10.5958/2322-0996.2017.00001.1

Rani, S. (2016). *Introduction :* -. *4*(7), 477–486. https://doi.org/10.21474/IJAR01

Rasul, A., Akhtar, N., Khan, B. A., Mahmood, T., Uz Zaman, S., & Shoaib Khan, H. M. (2012). Formulation development of a cream containing fennel extract: In vivo evaluation for anti-aging effects. *Pharmazie*, *67*(1), 54–58. https://doi.org/10.1691/ph.2012.1083

Rather, M. A., Dar, B. A., Sofi, S. N., Bhat, B. A., & Qurishi, M. A. (2016). Foeniculum vulgare: A comprehensive review of its traditional use, phytochemistry, pharmacology, and safety. *Arabian Journal of Chemistry*, *9*, S1574–S1583. https://doi.org/10.1016/j.arabjc.2012.04.011

Rawat, M. (2016). a Review on Green Synthesis and Characterization of Silver Nanoparticles

and Their Applications: a Green Nanoworld. *World Journal of Pharmacy and Pharmaceutical Sciences*, *5*(7), 730–762. https://doi.org/10.20959/wjpps20167-7227

Raza, M. A., Kanwal, Z., Rauf, A., Sabri, A. N., & Riaz, S. (n.d.). *Size- and Shape-Dependent Antibacterial Studies of Silver Nanoparticles Synthesized by Wet Chemical Routes*. https://doi.org/10.3390/nano6040074

Reverberi, A. Pietro, Vocciante, M., Salerno, M., Ferretti, M., & Fabiano, B. (2019). *Green Synthesis of Silver Nanoparticles by Low-Energy Wet Bead Milling of Metal Spheres*.

Rodrı, L. (2000). *Electrochemical Synthesis of Silver Nanoparticles*. 9683–9688.

Roy, A., Bulut, O., Some, S., Mandal, A. K., & Yilmaz, M. D. (2019). Green synthesis of silver nanoparticles: Biomolecule-nanoparticle organizations targeting antimicrobial activity. *RSC Advances*, *9*(5), 2673–2702. https://doi.org/10.1039/c8ra08982e

Salem, J. K., El-Nahhal, I. M., Najri, B. A., & Hammad, T. M. (2016). Utilization of surface Plasmon resonance band of silver nanoparticles for determination of critical micelle concentration of cationic surfactants. *Chemical Physics Letters*, *664*, 154–158. https://doi.org/10.1016/j.cplett.2016.10.025

Salem, S. S., & Fouda, A. (2021). Green Synthesis of Metallic Nanoparticles and Their Prospective Biotechnological Applications: an Overview. *Biological Trace Element Research*, *199*(1), 344–370. https://doi.org/10.1007/s12011-020-02138-3

Salmen, S. H., & Alharbi, S. A. (2020). Silver nanoparticles synthesized biogenically from Aloe fleurentiniorum extract: characterization and antibacterial activity. *Green Chemistry Letters and Reviews*, *13*(1), 1–5. https://doi.org/10.1080/17518253.2019.1707883

Salunke, B. K., Sawant, S. S., Beom, S. L., & Kim, S. (2016). Microorganisms as efficient biosystem for the synthesis of metal nanoparticles : current scenario and future possibilities. *World Journal of Microbiology and Biotechnology*. https://doi.org/10.1007/s11274-016-2044-1

Samuel, M. S., Jose, S., & Selvarajan, E. (2019). Jo u rn Pr. *Journal of Photochemistry & Photobiology, B: Biology*, 111642. https://doi.org/10.1016/j.jphotobiol.2019.111642

Sankar, R., Karthik, A., Prabu, A., Karthik, S., Shivashangari, K. S., & Ravikumar, V. (2013). Origanum vulgare mediated biosynthesis of silver nanoparticles for its antibacterial and

anticancer activity. *Colloids and Surfaces B: Biointerfaces*, *108*, 80–84. https://doi.org/10.1016/j.colsurfb.2013.02.033

Saravanan, M., Arokiyaraj, S., Lakshmi, T., & Pugazhendhi, A. (2018). Synthesis of silver nanoparticles from Phenerochaete chrysosporium (MTCC-787) and their antibacterial activity against human pathogenic bacteria. *Microbial Pathogenesis*, *117*(February), 68–72. https://doi.org/10.1016/j.micpath.2018.02.008

Saygi, K. O., & Cacan, E. (2021). Antioxidant and cytotoxic activities of silver nanoparticles synthesized using Tilia cordata flowers extract. *Materials Today Communications*, *27*(December 2020), 102316. https://doi.org/10.1016/j.mtcomm.2021.102316

Shahat, A. A., Ibrahim, A. Y., Hendawy, S. F., Omer, E. A., Hammouda, F. M., Abdel-Rahman, F. H., & Saleh, M. A. (2011). Chemical composition, antimicrobial and antioxidant activities of essential oils from organically cultivated fennel cultivars. *Molecules*, *16*(2), 1366–1377. https://doi.org/10.3390/molecules16021366

Shaikh, J. R., & Patil, M. (2020). Qualitative tests for preliminary phytochemical screening: An overview. *International Journal of Chemical Studies*, *8*(2), 603–608. https://doi.org/10.22271/chemi.2020.v8.i2i.8834

Shrivas, K., Sahu, S., Patra, G. K., Jaiswal, N. K., & Shankar, R. (2016). Localized surface plasmon resonance of silver nanoparticles for sensitive colorimetric detection of chromium in surface water, industrial waste water and vegetable samples. *Analytical Methods*, *8*(9), 2088–2096. https://doi.org/10.1039/c5ay03120f

Siddiqi, K. S., Husen, A., & Rao, R. A. K. (2018). A review on biosynthesis of silver nanoparticles and their biocidal properties. *Journal of Nanobiotechnology*. https://doi.org/10.1186/s12951-018-0334-5

Siegel, J., Lyutakov, O., Rybka, V., Kolská, Z., & Švorčík, V. (2011). Properties of gold nanostructures sputtered on glass. *Nanoscale Research Letters*, *6*(1), 1–9. https://doi.org/10.1186/1556-276X-6-96

Singh, J., Dutta, T., Kim, K. H., Rawat, M., Samddar, P., & Kumar, P. (2018). "Green" synthesis of metals and their oxide nanoparticles: Applications for environmental remediation. *Journal of Nanobiotechnology*, *16*(1), 1–24. https://doi.org/10.1186/s12951-

018-0408-4

Singh, P., Kim, Y. J., Zhang, D., & Yang, D. C. (2016). Biological Synthesis of Nanoparticles from Plants and Microorganisms. *Trends in Biotechnology*, *34*(7), 588–599. https://doi.org/10.1016/j.tibtech.2016.02.006

Singh, S., Bharti, A., & Kumar, V. (2014). *Structural , thermal , zeta potential and electrical properties of disaccharide reduced silver nanoparticles*. *Di*, 2–7. https://doi.org/10.1007/s10854-014-2085-x

Sinha, S. N., & Paul, D. (2015). Phytosynthesis of silver nanoparticles using andrographis paniculata leaf extract and evaluation of their antibacterial activities. *Spectroscopy Letters*, *48*(8), 600–604. https://doi.org/10.1080/00387010.2014.938756

Siva Kumar, S., Rao, V. R., & Rao, G. N. (2013). Efficient Photocatalytic Degradation of Alizarin Red S by Silver-Impregnated Zinc Oxide. *Proceedings of the National Academy of Sciences, India Section A: Physical Sciences*, *83*(4), 309–315. https://doi.org/10.1007/s40010-013-0097-1

Sivakumar, S. R., Sasikala, C., & Sheela, T. (2018). *Bio- Synthesis Of Silver Nanoparticles From Leaf Extracts Of Martynia Annua L . And Its Antimicrobial Activity* . *7*(4), 40–47.

Swain, A. K. (2016). Review on Green Synthesis of Silver Nanoparticles by Physical, Chemical and Biological Methods. *International Journal of Scientific & Engineering Research*, *7*(10), 551–554. https://doi.org/10.14299/ijser.2016.10.008

Thangavelu, S., Kumar, R. R., & Gopal, S. (2018). *Green synthesis of silver nanoparticles using galinsoga parviflora leaf extract and its antibacterial and antioxidant activities*. *November*.

Thiagarajan, S., Sanmugam, A., & Vikraman, D. (2017). Facile Methodology of Sol-Gel Synthesis for Metal Oxide Nanostructures. *Recent Applications in Sol-Gel Synthesis*, 1–16. https://doi.org/10.5772/intechopen.68708

Thompson, D. J., & Lowe, C. D. (2011). *Field estimates of reproductive success in a model insect : behavioural surrogates are poor predictors of fitness*. 905–913. https://doi.org/10.1111/j.1461-0248.2011.01655.x

Tomaszewska, E., Soliwoda, K., Kadziola, K., Tkacz-szczesna, B., Celichowski, G.,

Cichomski, M., Szmaja, W., & Grobelny, J. (2013). *Tomaszewska2013.Pdf*. *2013*.

Tomaszewska, E., Soliwoda, K., Kadziola, K., Tkacz-Szczesna, B., Celichowski, G., Cichomski, M., Szmaja, W., & Grobelny, J. (2013). Detection limits of DLS and UV-Vis spectroscopy in characterization of polydisperse nanoparticles colloids. *Journal of Nanomaterials*, *2013*. https://doi.org/10.1155/2013/313081

Tsuji, T. (2002). Preparation of silver nanoparticles by laser ablation in solution. *Applied Surface Science*, *202*(1–2), 80–85.

Vanlalveni, C., Rajkumari, K., Biswas, A., Adhikari, P. P., & Lalfakzuala, R. (2018). *Green Synthesis of Silver Nanoparticles Using Nostoc linckia and its Antimicrobial Activity : a Novel Biological Approach*.

Vega-Baudrit, J., Gamboa, S. M., Rojas, E. R., & Martinez, V. V. (2019). Synthesis and characterization of silver nanoparticles and their application as an antibacterial agent. *International Journal of Biosensors & Bioelectronics*, *5*(5). https://doi.org/10.15406/ijbsbe.2019.05.00172

Vishwanath, R., & Negi, B. (2021). Conventional and green methods of synthesis of silver nanoparticles and their antimicrobial properties. *Current Research in Green and Sustainable Chemistry*, *4*(October), 100205. https://doi.org/10.1016/j.crgsc.2021.100205

Widyaningtyas, A. L., Yulizar, Y., & Apriandanu, D. O. B. (2019). Ag2O nanoparticles fabrication by Vernonia amygdalina Del. leaf extract: Synthesis, characterization, and its photocatalytic activities. *IOP Conference Series: Materials Science and Engineering*, *509*(1). https://doi.org/10.1088/1757-899X/509/1/012022

Yaqoob, A. A., Umar, K., & Ibrahim, M. N. M. (2020). Silver nanoparticles: various methods of synthesis, size affecting factors and their potential applications–a review. *Applied Nanoscience (Switzerland)*, *10*(5), 1369–1378. https://doi.org/10.1007/s13204-020-01318-w

Yaseen, M., Ahmad, M., Wani, T. A., Ahmad, M., Gani, B. A., & Qureshi, R. (2017). Phytochemical screening and antioxidant activity of extracts of the leaf and stem of Achillea millefolium. *International Journal of Advanced Science and Research*, *2*(6), 55–59.

Yusuf, M. (2019). *Silver Nanoparticles: Synthesis and Applications*. 2343–2356.

Zhang, X. F., Liu, Z. G., Shen, W., & Gurunathan, S. (2016). Silver nanoparticles: Synthesis, characterization, properties, applications, and therapeutic approaches. *International Journal of Molecular Sciences*, *17*(9). https://doi.org/10.3390/ijms17091534

Zodrow, K., Brunet, L., Mahendra, S., Li, D., Zhang, A., Li, Q., & Alvarez, P. J. J. (2009). Polysulfone ultrafiltration membranes impregnated with silver nanoparticles show improved biofouling resistance and virus removal. *Water Research*, *43*(3), 715–723. https://doi.org/10.1016/j.watres.2008.11.014